

Cranial Anatomy of the Extinct Amphisbaenian *Rhineura hatcherii* (Squamata, Amphisbaenia) Based on High-Resolution X-Ray Computed Tomography

Maureen Kearney,^{1*} Jessica Anderson Maisano,² and Timothy Rowe³

¹Department of Zoology, Field Museum of Natural History, Chicago, Illinois 60605

²Jackson School of Geosciences, The University of Texas at Austin, Austin, Texas 78712

³Jackson School of Geosciences and Texas Memorial Museum, The University of Texas at Austin, Austin, Texas 78712

ABSTRACT The fossilized skull of a small extinct amphisbaenian referable to *Rhineura hatcherii* Baur is described from high-resolution X-ray computed tomographic (HRXCT) imagery of a well-preserved mature specimen from the Brule Formation of Badlands National Park, South Dakota. Marked density contrast between bones and surrounding matrix and at bone-to-bone sutures enabled the digital disarticulation of individual skull elements. These novel visualizations provide insight into the otherwise inaccessible three-dimensionally complex structure of the bones of the skull and their relationships to one another, and to the internal cavities and passageways that they enclose. This study corrects several previous misidentifications of elements in the rhineurid skull and sheds light on skull construction generally in “shovel-headed” amphisbaenians. The orbitosphenoids in *R. hatcherii* are paired and entirely enclosed within the braincase by the frontals; this is in contrast to the condition in many extant amphisbaenians, in which a large zygous orbitosphenoid occupies a topologically distinct area of the skull, closing the anterolateral braincase wall. *Rhineura hatcherii* retains a vestigial jugal and a partially fused squamosal, both of which are absent in many extant species. Sculpturing on the snout of *R. hatcherii* represents perforating canals conveying sensory innervation; thus, the face of *R. hatcherii* receives cutaneous innervation to an unprecedented degree. The HRXCT data (available at www.digimorph.org) corroborate and extend previous hypotheses that the mechanical organization of the head in *Rhineura* is organized to a large degree around its burrowing lifestyle. *J. Morphol.* 000:000–000, 2005.

© 2004 Wiley-Liss, Inc.

KEY WORDS: Squamata; Amphisbaenia; Rhineuridae; *Rhineura hatcherii*; cranial anatomy; computed tomography; White River Group; worm lizards

Amphisbaenians (“worm lizards”) are a poorly known clade of fossorial reptiles including roughly 150 extant species, nearly all of which are limbless (Gans, 1978). Many members of the clade lie within or near the smallest order of vertebrate size magnitudes (McMahon and Bonner, 1983), and their size alone presents a daunting impediment to detailed morphological analysis. Because of the destructive

nature of serial sectioning and the intensive labor required to generate and interpret histological preparations in three dimensions (e.g., Olson, 1995), few amphisbaenian species have been described from sections. Moreover, extant amphisbaenians are all fossorial, elusive in the field, and generally poorly represented in museum collections, even in those countries that they inhabit today. As a result, both the structure and relationships of amphisbaenians are among the most problematic of any vertebrate clade. Compounding these difficulties is the highly derived nature of amphisbaenian anatomy, which makes comparisons to other squamate reptiles difficult.

In precladistic literature, amphisbaenian species were clustered into categories whose contents were based on combinations of phenetic features of the skeleton and scalation and/or on geographic similarities. Experts have traditionally referred to “shovel-headed” (e.g., *Rhineura*), “round-headed” (e.g., *Bipes*), “spade-headed” (e.g., *Diplometopon*), and “keel-headed” (e.g., *Anops*) amphisbaenian groups. The question of whether these groupings represent monophyletic lineages remains open. Higher-level relationships among amphisbaenians only recently have begun to be tested through phylogenetic methods. The first cladistic analysis of the group (Kearney, 2003) supported the monophyly of the “shovel-headed” rhineurids (including the extant *Rhineura floridana* and all fossil relatives) but exposed several problems, including the recognition of a basic morphological dichotomy between extant and fossil taxa.

Contract grant sponsor: NSF; Contract grant numbers: IIS-9874781, IIS-0208675 (to T.R.).

*Correspondence to: Maureen Kearney, Department of Zoology, Field Museum of Natural History, Chicago, IL 60605.
E-mail: mkearney@fieldmuseum.org

Published online in
Wiley InterScience (www.interscience.wiley.com)
DOI: 10.1002/jmor.10210

The vast majority of known fossil amphisbaenians are “shovel-headed,” and the lack of a fossil record for other morphologically derived lineages causes some difficulty in interpreting relationships.

Many problems that face morphology-based phylogenetic analysis of amphisbaenians will likely remain unsolved until more of the fundamental anatomy and variability among amphisbaenian species is documented. The skull of *Amphisbaena alba* (a “round-headed” species) was recently described in unprecedented detail (Montero and Gans, 1999), providing the first bone-by-bone account of an amphisbaenian skull. No other species is known in comparable detail, leaving us at present with a rather typological appreciation for the clade as a whole.

Additional challenges impede the interpretation of amphisbaenian fossils in particular. Knowledge of the amphisbaenian fossil record has grown gradually over the last century (e.g., Baur, 1893; Gilmore, 1928; Taylor, 1951; Berman, 1973, 1976; Estes, 1983). However, due to their small size, incomplete preservation, and encasement in rock matrix, the anatomy of fossil amphisbaenians has proven especially difficult to study in detail. The internal architecture of the snout, composition of the orbital wall, and geometry of the endocranial cavities are virtually inaccessible via traditional techniques, and many reported details of their anatomy appear to be speculative.

Fossil amphisbaenians are known mainly from a number of well-preserved skulls assignable to Rhineuridae (Berman, 1973, 1976; Gans, 1978; Estes, 1983; Kearney, 2003). The fossil record of rhineurids extends back to the Upper Paleocene (Estes, 1983) and is exclusively North American. There is a single surviving relict species, *Rhineura floridana*, occurring in north-central Florida and Georgia. Nearly all known fossil amphisbaenians are derived rhineurids with a stereotypical “shovel-headed” morphology in which the snout is dorsoventrally flattened and the skull exhibits a strong craniofacial angle. This anatomy is associated with the use of the head as a digging tool in a specialized, characteristic behavior in *R. floridana* (Gans, 1960, 1974). Rhineurid monophyly is corroborated by several synapomorphies such as a strong craniofacial angulation; a medial nasal process of the premaxilla that extends only slightly posteriorly in superficial view, not quite reaching the anterior edge of the frontal; pterygoid-vomer contact; a low premaxillary tooth count; a dentary process of the coronoid overlapping the dentary; and others (Kearney, 2003).

In this study, we used high-resolution X-ray computed tomography (HRXCT) (Rowe et al., 1997) to produce a detailed description of the anatomy of a fossil skull referable to *Rhineura hatcherii* Baur (but see caveats below). *Rhineura hatcherii* is a “shovel-headed” amphisbaenian known from some dozens of

specimens collected from Oligocene age terrigenous sediments of South Dakota, Nebraska, and Colorado (Estes, 1983). Several species of *Rhineura* have been named and the superficial anatomy of several partial skulls described (Gilmore, 1928; Taylor, 1951; Estes, 1983), but none is known in detail. We describe the structure of an especially well-preserved skull to provide the first thorough description of an extinct amphisbaenian as well as a general morphological characterization of the “shovel-headed” morph. By comparison with its extant relatives, this more detailed account of an Oligocene species reveals new insight into the peculiarities of amphisbaenian cranial architecture. We also present additional character data for comparison among amphisbaenians generally, with the anticipation that they will contribute to greater resolution of amphisbaenian phylogeny.

MATERIALS AND METHODS

This description is based primarily on a single skull of *Rhineura hatcherii* (Fig. 1) collected from the Brule Formation (Orellan) in Cottonwood Pass, Badlands National Park, South Dakota (BADL 18306; formerly SDSM V2000-01/3040). The skull is nearly complete, undistorted, and well preserved, with the mandible closely joined to the cranium. It was buried in a poorly sorted clastic matrix of clay, silt, and sand particles. Most of the matrix originally encasing the specimen was mechanically prepared away from its outer surface, but portions of the skull, such as the dentary teeth and palate, remain obscured, as do all internal cavities. All cranial elements except the extracolumella and hyobranchial apparatus are present. However, both nasal bones and the dorsal edges of the underlying septomaxillae are eroded completely through, exposing the nasal passageway. Bilaterally symmetrical holes perforating the parietal and otic-occipital complex, and truncation of parts of the basicranium and the superior edges of the mandibles, appear to represent damage incurred during mechanical preparation of the specimen.

While studying the primary specimen (Fig. 1), we compared it to several other *Rhineura hatcherii* specimens from the same region and formation (BADL 11414 [formerly SDSM V998/43412]; BADL 11415 [formerly SDSM V998/43413]; and BADL 11416 [formerly V675/43414]). These comparisons aided in the identification of weathering and mechanical preparation artifacts in the described specimen.

The specimen (Figs. 1, 6) is referable to *Rhineura hatcherii* based on its unique dentition, jaw, and suspensorium. Diagnostic features include the presence of up to seven maxillary and dentary teeth, a postcoronoid region of the mandible approximately equal in length to the precoronoid region, and the placement of the occipital condyle in an unelevated position (Gilmore, 1928; Taylor, 1951; Estes, 1983). Whether this diagnosis is adequate to distinguish *R. hatcherii* from all other named species of *Rhineura*, most of which are based on fragmentary material, remains to be tested (Kearney, 2003). There are two spellings of the species name in the literature, and we employ the original spelling (*R. hatcherii*) (Baur, 1893) rather than the more commonly but informally accepted, corrected spelling (*R. hatcheri*) (Gilmore, 1928; Estes, 1983).

Anatomical nomenclature for amphisbaenian cranial anatomy is inconsistent and revision of this nomenclature is beyond the scope of the present work. However, insofar as naming conventions can present barriers to proper comparison and subsequent identification of homologies (Rowe, 1986), we attempt to implement an explicit, consistent terminology throughout the description and figure labels. For convenience and clarity, we generally avoid employing the same cardinal direction terminology (anter-



Fig. 1. *Rhineura hatcherii* (BADL 18306). Photographic images of the specimen in (A) lateral and (C) ventral views, and three-dimensional reconstructions based on HRXCT data in (B) lateral and (D) ventral views. Scale bar = 1 mm. Note the clear distinction between bone and matrix in the HRXCT reconstructions.

ior, posterior, dorsal, ventral, medial, lateral) as both the names of anatomical structures (as adjectives) and as descriptors of those structures (as adverbs). Familiar names of bones and openings imply homology with elements of the same name in other squamates, except where noted below.

The description of the specimen is based on HRXCT imagery generated at the High-Resolution X-ray CT Facility at The University of Texas at Austin. The scanning parameters were as follows. A Feinfocus microfocal X-ray source operating at 150 kV and 0.16 mA with no X-ray prefilter was employed. An air wedge was used as the specimen was scanned in 160% offset mode. Slice thickness corresponded to 4 lines in a CCD image intensifier imaging system, with a source-to-object distance of 16 mm. For each slice, 2,400 views were taken with three samples per view. The field of image reconstruction was 7.5 mm, and an image reconstruction offset of 500 was used with a reconstruction scale of 2. The specimen was scanned in three-slice mode, in which three slices were collected simultaneously during a single specimen rotation.

The dataset consists of 414 transverse (=coronal) CT slices taken along the long axis of the skull from the tip of the snout to the occiput (Figs. 2, 3). Each slice image was gathered at 512×512 pixels resolution, with an in-plane resolution of $15 \mu\text{m}$ per pixel. Each slice represents a thickness of $37 \mu\text{m}$, with $37 \mu\text{m}$ interslice spacing. The dataset was digitally resliced along the other two orthogonal axes—frontal (=horizontal; from top to bottom) and sagittal (from left to right)—using NIH Image (National Institutes of Health). Labeled sample CT slices along all three orthogonal axes are presented in Figures 3–5.

High density contrast between the fossilized bone and most matrix particles permitted unambiguous identification of the bone–matrix interface and boundaries between individual bones. It also facilitated digital segmentation of the data volume, in which nearly all matrix particles were digitally “removed” or rendered transparent, permitting for the first time the examination of all surfaces and spaces within the skull. High density contrast also enabled digital “removal” of the mandible from the cranium (Fig. 6C), revealing the bones of the palate, and digital “explosion” of the skull so that each element could be rendered and described separately (Figs. 7–26). For paired elements, the left element was isolated unless the right element was better preserved; in these cases (septomaxilla, nasal, quadrate, stapes, and mandible) right elements were mirrored to maintain consistency in spatial orientation in the figures. Isolation of individual bones from the data volume was performed on a consecutive slice-by-slice basis using Adobe PhotoShop (San Jose, CA). The three-dimensional reconstructions of the skull and isolated elements were generated in VoxBlast (Vaytek, Fairfield, IA). The cranial bones and mandible are described separately.

The reconstructions presented here may be interpreted much as if they were photographs. However, they actually represent density maps of the segmented specimen volume in which lighter grayscales represent denser materials (bone) and darker grayscales represent less dense materials (air, matrix). Some of the sand-sized matrix particles include metallic oxides and other materials that approach or exceed the density of the fossilized bone. These particles appear on the images as small, bright pixels.

The skull as a whole (Fig. 6) is described first, followed by each individual cranial element in isolation (Figs. 7–26). The CT slices spanned by each element are noted at the beginning of the description of that element, and labeled representative CT slices (Figs. 2–5) illustrate the internal anatomy of the skull in transverse (Tra), sagittal (Sag), and frontal (Fro) slice planes.

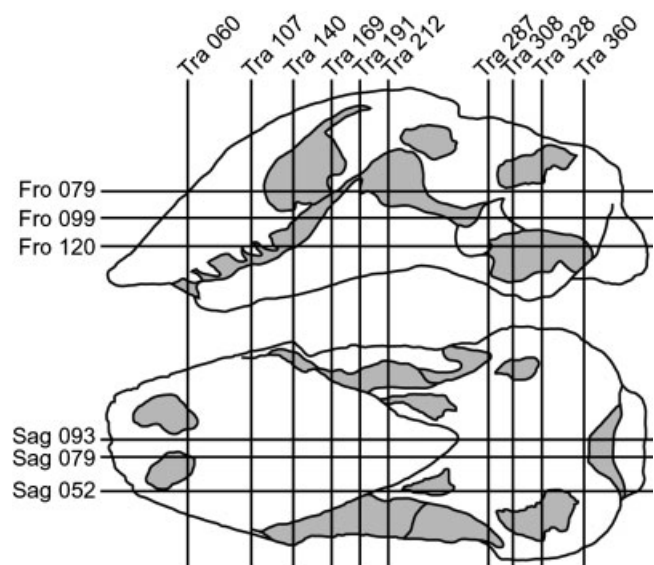


Fig. 2. Diagram showing relative positions and orientations of sample CT slices shown in Figures 3–5.



Figure 3

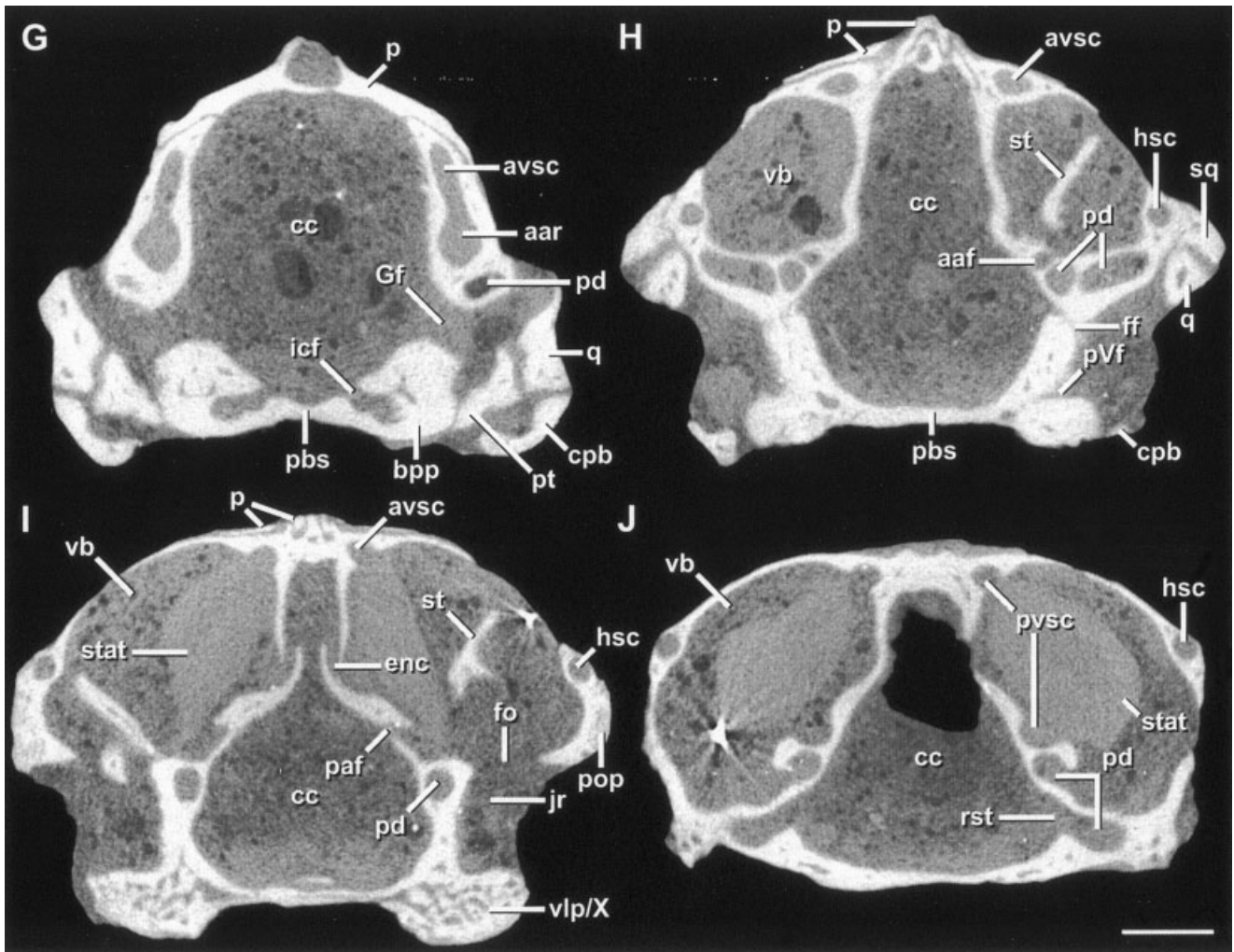


Figure 3. (Continued)

Fig. 3. *Rhineura hatcherii* (BADL 18306). Selected transverse (Tra) CT slices. (A) Tra 60, (B) Tra 107, (C) Tra 140, (D) Tra 169, (E) Tra 191, (F) Tra 212, (G) Tra 287, (H) Tra 308, (I) Tra 328, (J) Tra 360. Scale bar = 1 mm. aaf, anterior auditory foramen; aar, anterior ampullary recess; af, apical foramen; appr, alar process of prootic; avsc, anterior vertical semicircular canal; bpp, basiptyergoid process; cc, cranial cavity; chv, choanal vault; co, coronoid; cpb, compound bone; dn, dentary; dnt, dentary tooth; ec, ectopterygoid; enc, endolymphatic canal; f, frontal; fc, frontal canal; ff, facial foramen; fo, fenestra ovale; Gf, Gasserian foramen; hsc, horizontal semicircular canal; icf, internal carotid foramen; j, jugal; jr, jugular recess; lf, labial foramen; m, maxilla; Mc, Meckelian canal; mt, maxillary tooth; n, nasal; ncf, nasal communicating foramen; nf, nutritive foramen; orb, orbit; os, orbitosphenoid; p, parietal; paf, posterior auditory foramen; pal, palatine; pbs, parabasisphenoid; pc, pulp cavity; pd, perilymphatic duct; pf, prefrontal; pm, premaxilla; pop, paroccipital process; pt, pterygoid; pVf, posterior Vidian foramen; pvsc, posterior vertical semicircular canal; q, quadrate; rst, recessus scala tympani; sm, septomaxilla; sp, splenial; sq, squamosal; st, stapes; stat, statolith mass; v, vomer; vb, vestibule; vf, vomerine foramen; vlp, ventrolateral process; X, "Element X."

An interactive, web-deliverable version of the original HRXCT dataset keyed to the slice numbers referenced below, as well as animations of all isolated bones, can be viewed at http://www.digimorph.org/specimens/Rhineura_hatcherii, and the original full-resolution HRXCT data are available from the authors.

RESULTS

Overview of Skull (Figs. 1, 6)

The skull of *Rhineura hatcherii* displays a characteristic postorbital elongation and preorbital shortening seen in almost all amphisbaenians. The skull measures 15.6 mm from the tip of the snout to the posterior tip of the occipital condyle, and 6.9 mm at its widest expanse, at the level of the external opening of the jugular recess. The skull is prognathous and displays the typical rhineurid condition, in which the snout projects sharply anterior to the mouth and significantly overhangs the mandible. Other amphisbaenians have a sharp snout, but in the "shovel-headed" rhineurids it forms a broad

wedge whose leading edge is oriented horizontally, protruding beyond the borders of the nares.

For descriptive purposes, the skull can be divided into facial and cranial segments, with a strong craniofacial deflection angle delimiting the two at the frontoparietal suture. Along this border, the frontals and parietal interdigitate in a complex, three-dimensional syndesmosis. The facial segment of the skull is composed of the premaxilla, septomaxilla, maxilla, nasal, frontal, prefrontal, part of the parietal, and the palatal elements. The median premaxilla and paired nasals are dorsoventrally flattened to form the sharp leading edge or rostral blade of the shovel snout. This blade is buttressed laterally on each side by the maxilla, which contacts the nasal in a tongue-and-groove suture, and by palatal elements, which ultimately transmit rostral loads to the basipterygoid processes. The rostral blade is also heavily buttressed against the braincase via a median strut of complex structure that includes contributions from the premaxilla, septomaxilla, maxilla, vomer, and palatine.

Together, the premaxilla, septomaxilla, maxilla, and nasal form the border around the ventrally opening external naris. As in other "shovel-headed" amphisbaenians, the nares in *Rhineura hatcherii* open through the ventral surface of the snout anterior to the mouth, in contrast to the anterolateral opening in most other forms. The maxilla comprises most of the face as it forms the lateral wall and a partial floor beneath the nasal chamber. The nasal and the underlying portion of the septomaxilla, which are eroded almost entirely away on both sides of the specimen, form the roof of the nasal chamber. The nasal extends posteriorly over the frontal as a sharp lappet that tapers to a point and ends nearly level with the anterior orbital rim. It fits into a V-shaped depression in the anterior margin of the adjacent frontal, such that the right and left nasofrontal sutures together are W-shaped. The preserved medial portions of both nasals lie in contact on the midline, surrounding the nasal process of the premaxilla and obscuring most of it from view. Most of the outer surfaces of the facial segment are sculptured by pits and grooves, which are most conspicuous on the frontal, maxilla, and nasal; the CT sections (Figs. 3–5) show these to be continuous with canals that likely carried vasculature and cutaneous sensory branches of the trigeminal nerve. They suggest the presence of cutaneous innervation over the entire facial segment of the skull to a much greater degree than that seen in other squamates (Oelrich, 1956).

The orbit lies entirely within the facial segment of the skull, where it faces laterally, and is deeply inset beneath the overhanging frontal. The orbital wall is formed anteriorly by the prefrontal and the descending process of the frontal, while the maxilla, ectopterygoid, and palatine contribute to the orbital floor. The eye almost certainly was vestigial and

functionless, and covered with an outer arcade of scales (Cope, 1900; Gilmore, 1928; Gans, 1960). In the closest living relative, *Rhineura floridana*, the eye is vestigial and buried deeply within the orbit beneath two supraciliary scales and one preorbital scale (Eigenmann, 1902). The eyeball of this living species lacks a distinctive fibrous layer and there is no trace of an organized, compact optic nerve in the orbit, although its fibrous sheath and pigment cells mark its former pathway (Eigenmann, 1902). Moreover, as in *R. hatcherii*, in *R. floridana* there is no evident communication between the orbit and cranial cavity that could have transmitted an optic nerve. Additionally, the Harderian gland is greatly hypertrophied and engulfs the eyeball as it fills the orbit in *R. floridana*. All of these features suggest that the eye was virtually functionless as a sensory organ in *R. hatcherii*. The bony orbital rim is incomplete posteriorly, where it merges with the lateral wall of the braincase. No postorbital arch is preserved in this specimen, nor are there any published descriptions of this structure in any species of *Rhineura*. However, a vestigial jugal has been noted in *R. floridana* (Zangerl, 1944; Vanzolini, 1951) and *R. hatcherii* (Baur, 1893), and one is present in the specimen described here (see below).

The palate lacks dentition and is surrounded on three sides by the upper dentition. There are three teeth in the azygous premaxilla and six teeth in each maxilla, which are met by seven teeth in each dentary. The palate is formed by the premaxilla, maxilla, pterygoid, ectopterygoid, palatine, and vomer. There is no palatal vacuity, and the pyriform recess is narrow and roofed by a long parabasisphenoid cultriform process. The fenestra vomeronasalis is large and bounded by the vomer posteromedially, the premaxilla anteriorly, and the maxilla laterally. This passageway communicates with a voluminous vomeronasal (Jacobson's) chamber. The premaxilla, nasal septomaxilla, and vomer all contribute to a complex internasal septum, which divides the nasal chamber into right and left passageways to the level of the fourth maxillary tooth posteriorly.

In *Rhineura hatcherii*, as in other amphisbaenians, the cranial segment of the mature skull consists largely of the parietal and a single continuous element known as the occipital complex. The latter is composed of bones that develop from separate ossification centers and that generally remain separate throughout at least a portion of postnatal ontogeny in other squamates, including the median supraoccipital and basioccipital and the paired exoccipital and prootic (Montero et al., 1999). In *Rhineura*, these bones also fuse together with the ossification centers of the otic capsule and basicranial axis (parabasisphenoid) to form the adult otic-occipital complex.

The roof of the cranial segment is formed anteriorly by the azygous parietal. A sagittal crest extends along the parietal from the point of deflection, over



Fig. 4. *Rhineura hatcherii* (BADL 18306). Selected sagittal (Sag) CT slices. (A) Sag 052, (B) Sag 079, (C) Sag 093. Scale bar = 1 mm. aar, anterior ampullary recess; appr, alar process of prootic; avsc, anterior vertical semicircular canal; bpp, basipterygoid process; cc, cranial cavity; cvcp, cavum epiptericum; dc, dental canal; dn, dentary; dnt, dentary tooth; ec, ectopterygoid; f, frontal; fcf, facial communicating foramen; fm, foramen magnum; fvo, fenestra vomeronasalis; m, maxilla; Mc, Meckelian canal; mt, maxillary tooth; n, nasal; nf, nutritive foramen; occ, occipital condyle; ooc, otic-occipital complex; os, orbitosphenoid; p, parietal; pal, palatine; par, posterior ampullary recess; pas, processus ascendens of supraoccipital; pbs, parabasisphenoid; pc, pulp cavity; pd, perilymphatic duct; pf, prefrontal; pm, premaxilla; pt, pterygoid; ptr, palatal trough; pvsc, posterior vertical semicircular canal; rc, rostral canal; rcc, recessus crus communis; sm, septomaxilla; sp, splenial; st, stapes; stat, statolith mass; v, vomer; vlp, ventrolateral process; X, "Element X."

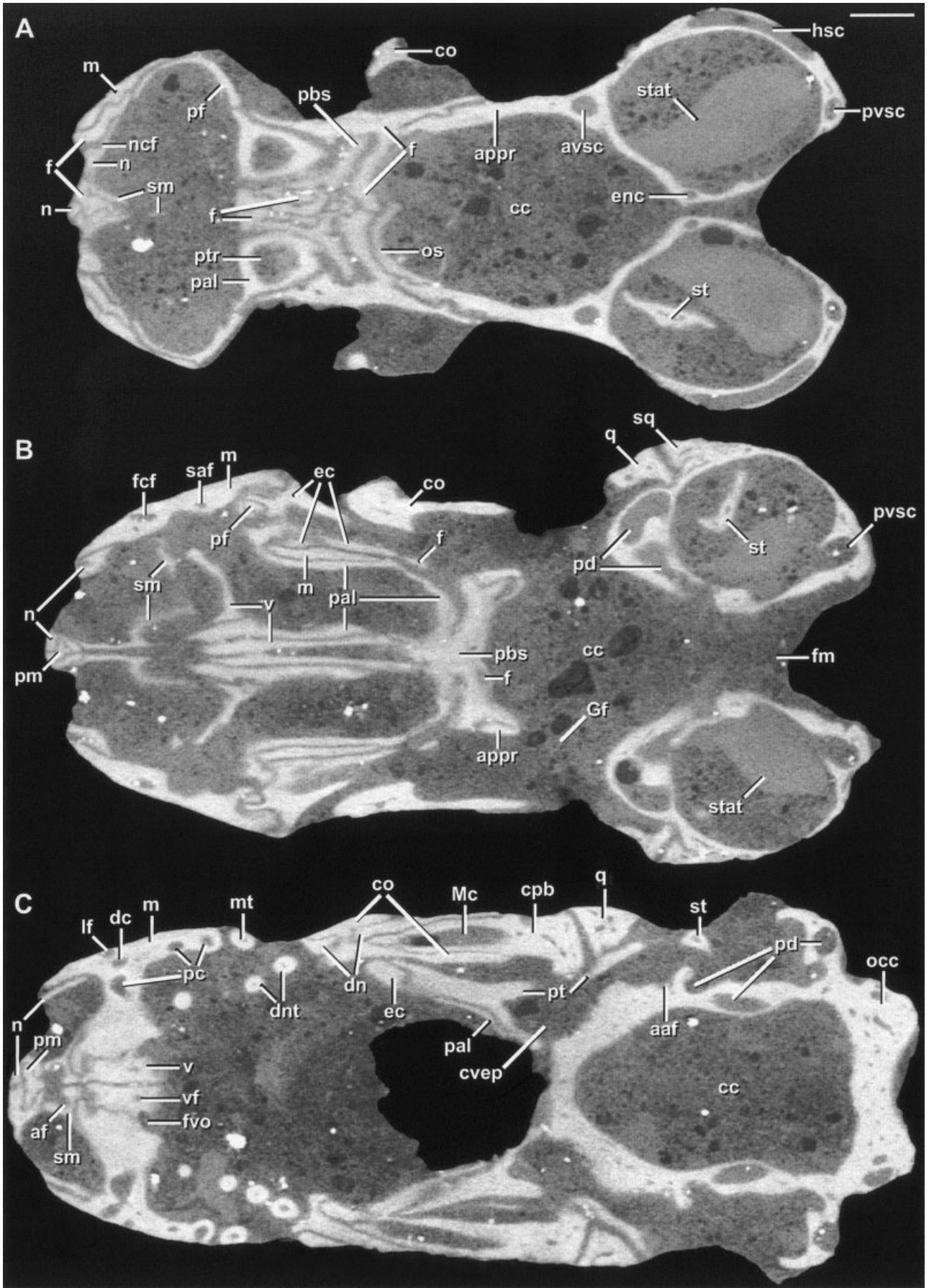


Figure 5

the dorsal surface of the otic–occipital complex, nearly to the foramen magnum. The cranial segment is widest across the otic region, at the level of the paroccipital processes, and tapers anteriorly to its narrowest constriction near the point of deflection between the cranial and facial segments. The otic capsule is proportionally very large. A large entity of uncertain homology known as Element X (Zangerl, 1944; Montero and Gans, 1999) is discernible distally capping the ventrolateral process of the basi-cranium (see Otic–Occipital Complex, below). The foramen magnum is weakly triangular, with a tall notch incising its dorsal edge. The occipital condyle is bicipital, roughly dumbbell-shaped, and greatly enlarged relative to the size of the skull when compared to most other amphisbaenians.

The occipital complex is entirely open and unenclosed by bones of the upper temporal arch, in contrast to the condition in most nonfossorial squamates. However, the adductor musculature was almost certainly bounded laterally by an arcade of large cephalic scales, as in *Rhineura floridana* (Eigenmann, 1902). A vestigial squamosal is present, but it forms little more than a small bit of bone that is partially fused to the paroccipital process. The quadrate is a short, robust element. Its proximal end articulates loosely with the squamosal, otic capsule, and quadrate process of the pterygoid, forming a streptostylic suspension for the lower jaw. The distal articulation of the quadrate is positioned anteromedially, where it forms a complex ginglymoid articulation with the mandible.

The mandible is a robust compound structure that supports seven dentary teeth on each side. With jaws closed, the mandibular teeth lie entirely medial to the maxillary teeth and posterior to the premaxillary teeth, and there is no contact between upper and lower dentitions. The dentaries remain unfused where they meet at the anterior midline. The mandibles are set far posterior to the tip of the overhanging snout and the external nares. Behind the tooth row, the mandible bears a tall coronoid process in a

mechanical configuration that most likely afforded a powerful bite (Gans, 1974).

Individual Elements of the Skull

Premaxilla (Fig. 7; Tra 002–085). The premaxilla in *Rhineura hatcherii* is an azygous element that is contacted on either side by the paired septomaxilla, nasal, maxilla, and vomer (Estes, 1983; Montero et al., 1999). In *Amphisbaena* the premaxilla is azygous throughout development, ossifying from a single median center (Montero et al., 1999). For comparative purposes, we describe the premaxilla as being organized around its alveolar plate (=basal plate of Montero and Gans, 1999), which in this specimen supports three tooth positions. Viewed ventrally, the alveolar plate is triangular and its teeth are arranged in a shallow V-shaped pattern (Fig. 7D). Judging from its alveolus, the subtheodont median tooth (missing in this specimen) was the most anterior tooth position and was by far the largest tooth implanted in the premaxilla, a condition characteristic of amphisbaenians generally (Gans, 1978; Estes et al., 1988; Kearney, 2003). The smaller, subpleurodont teeth on either side are more posteriorly placed and their crowns are directed posteroventrally to an extreme degree. There is no indication in the HRXCT data of replacement teeth developing at any of these three tooth loci. The alveolar plate of the premaxilla articulates with the maxilla on either side via a laterally tapering tongue that is grasped by a groove in the palatal process of the maxilla (Fig. 7A). This stands in contrast to the more elaborately interdigitating articulation between these bones in *A. alba* (Montero and Gans, 1999).

The alveolar plate projects forward to a narrow constriction, then broadens outward into its distinctive rostral process (Fig. 7D). This structure, which forms most of the rostral blade of the “shovel snout,” is entirely absent in some amphisbaenians (e.g., *Amphisbaena alba* [Montero and Gans, 1999]), and developed convergently in others (e.g., *Diplometopon*, *Pachycalamus* [Gans, 1960]). The rostral process is approximately as broad and long as the alveolar plate, thus the premaxilla is hour glass shaped and transversely constricted at its midpoint when viewed ventrally (Gilmore, 1928).

The nasal process of the premaxilla rises dorsally from the confluence between the rostral process and alveolar plate. Superficially, the nasal process appears to be short and peg-like (Fig. 6D). However, the CT imagery reveals that the nasal process arches over the narial cupola toward the frontal, and that its distal extremity is hidden from view by the medial edges of the right and left nasals, which meet along the superficial midline (Figs. 3A, 5C). The nasal process is widest at its base and tapers posteriorly to the point where it pinches out between the nasals.

Fig. 5. *Rhineura hatcherii* (BADL 18306). Selected frontal (Fro) CT slices. (A) Fro 079, (B) Fro 099, (C) Fro 120. Scale bar = 1 mm. aaf, anterior auditory foramen; af, apical foramen; appr, alar process of prootic; avsc, anterior vertical semicircular canal; cc, cranial cavity; co, coronoid; cpb, compound bone; cvcp, cavum epiptericum; dc, dental canal; dn, dentary; dnt, dentary tooth; ec, ectopterygoid; enc, endolymphatic canal; f, frontal; fcf, facial communicating foramen; fm, foramen magnum; fvo, fenestra vomeronasalis; Gf, Gasserian foramen; hsc, horizontal semicircular canal; lf, labial foramen; m, maxilla; Mc, Meckelian canal; mt, maxillary tooth; n, nasal; ncf, nasal communicating foramen; occ, occipital condyle; os, orbitosphenoid; pal, palatine; pbs, parabasisphenoid; pc, pulp cavity; pd, perilymphatic duct; pf, prefrontal; pm, premaxilla; pt, pterygoid; ptr, palatal trough; pvsc, posterior vertical semicircular canal; q, quadrate; saf, superior alveolar foramen; sm, septomaxilla; st, stapes; stat, statolith mass; sq, squamosal; v, vomer; vf, vomerine foramen.

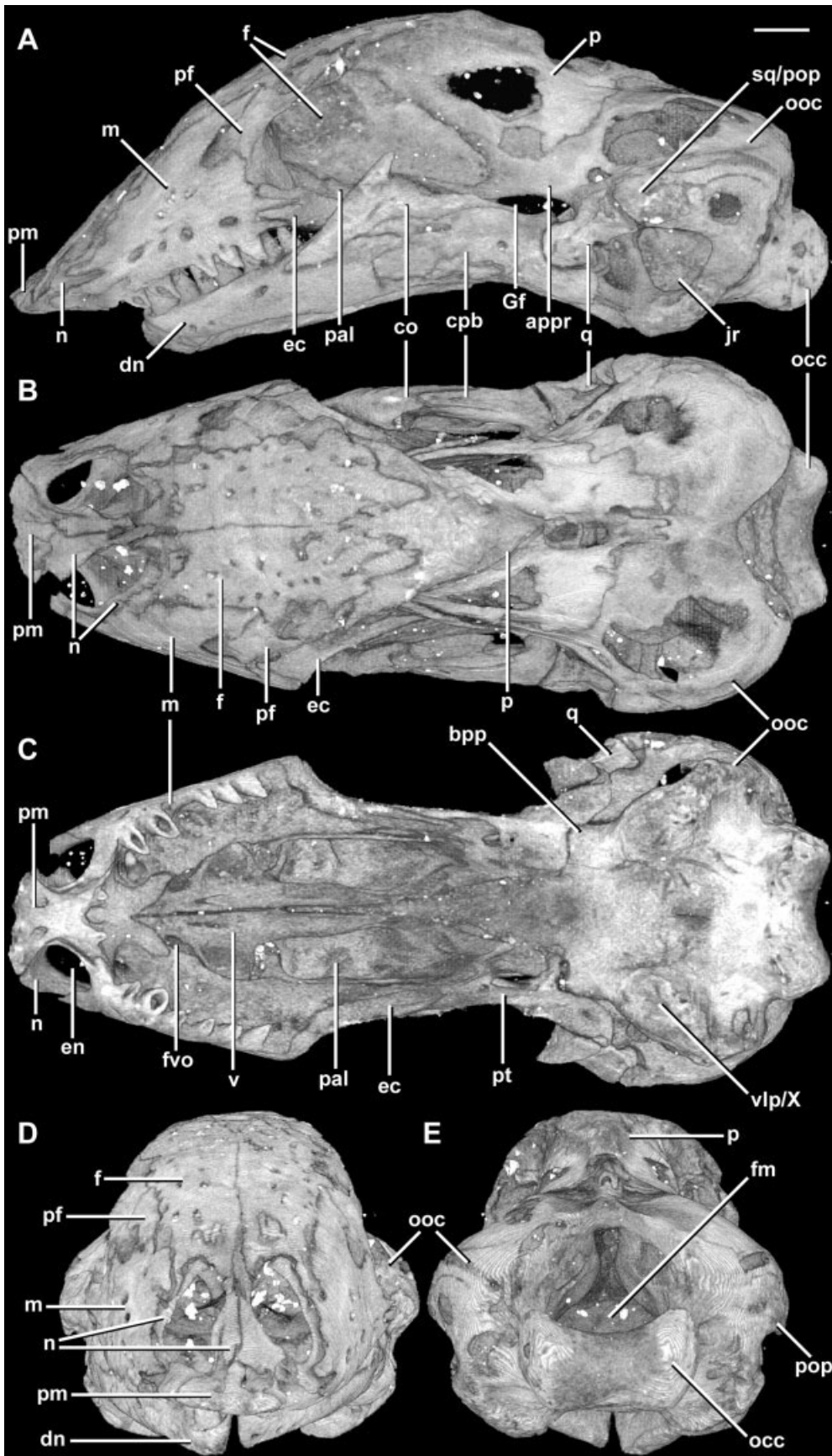


Fig. 6. *Rhineura hatcherii* (BADL 18306). Three-dimensional digital reconstruction of specimen with matrix rendered transparent in (A) lateral, (B) dorsal, (C) ventral (with mandible removed), (D) anterior, and (E) posterior views. Anterior to left in A–C. Scale bar = 1 mm. appr, alar process of prootic; bpp, basiptyergoid process; co, coronoid; cpb, compound bone; dn, dentary; ec, ectopterygoid; en, external naris; f, frontal; fm, foramen magnum; fo, fenestra ovale; fvo, fenestra vomeronasalis; Gf, Gasserian foramen; jr, jugular recess; m, maxilla; n, nasal; occ, occipital condyle; ooc, otic-occipital complex; p, parietal; pal, palatine; pf, prefrontal; pm, premaxilla; pop, paroccipital process; pt, pterygoid; q, quadrate; sm, septomaxilla; sq, squamosal; v, vomer; vlp, ventrolateral process; X, “Element X.”

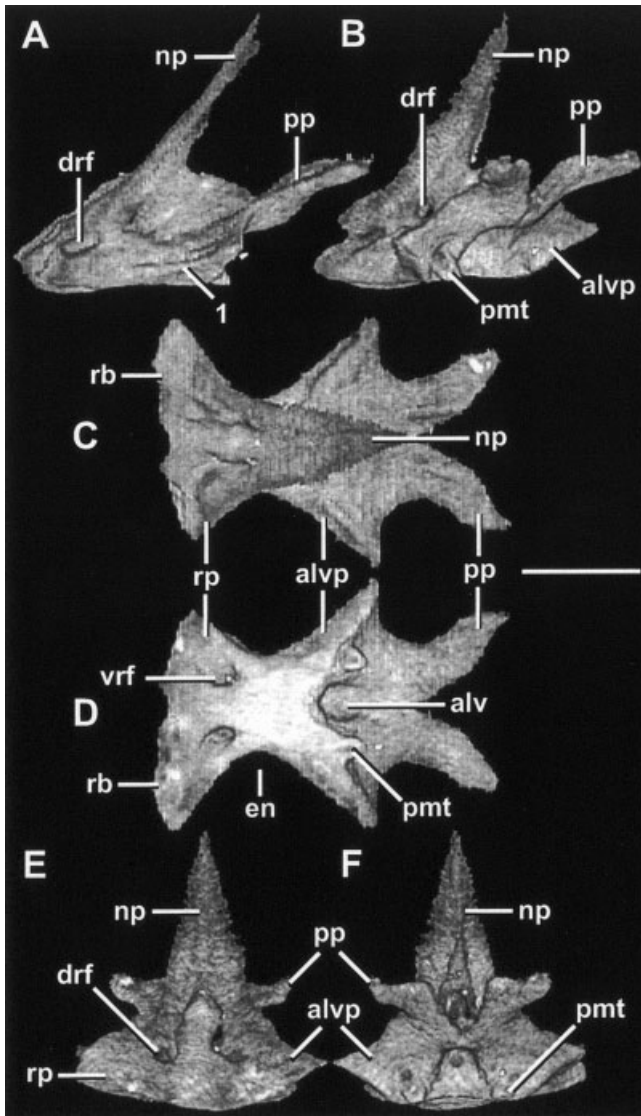


Fig. 7. Premaxilla in (A) lateral, (B) oblique lateral, (C) dorsal, (D) ventral, (E) anterior, and (F) posterior views. Anterior to left in A–D. Scale bar = 1 mm. alvp, alveolar plate; drf, dorsal rostral foramen; en, external naris; np, nasal process; pmt, premaxillary tooth; pp, palatal process; rb, rostral blade; rp, rostral process; vrf, ventral rostral foramen; 1, ridge clasped by nasal process of maxilla.

In most squamates the alveolar and nasal processes make substantial contributions to the narial border, while the superior surface of the alveolar plate forms the floor of the naris (Oelrich, 1956). This condition persists in *Amphisbaena alba* (Montero and Gans, 1999). However, in many “shovel-headed” amphisbaenians, including *Rhineura hatcherii*, the external naris is displaced anteroventrally such that it opens entirely from the ventral surface of the rostrum and has no floor (Fig. 6C). The premaxillary rostral process contributes to the narial border, but most of its circumference is built by a rostral spine of the maxilla and by the nasal (Tra

044). When viewed ventrally, the premaxilla can be seen to widely separate the external nares on the ventral face of the rostrum, but the narrow intervention by the maxillary rostral spine largely separates the premaxilla from the narial border.

The premaxilla is distinctly stepped just posterior to the naris, where it continues onto the palate as divergent palatal processes that extend to the level of the second maxillary tooth (Tra 085). The palatal process lies ventrolateral to the vomer and fits into an impression on the inferior surface of the maxilla (Fig. 4B). The palatal process is absent or weakly developed in many non-rhineurid amphisbaenians (Kearney, 2003).

The premaxilla is penetrated by a short rostral canal (=longitudinal canal of Montero and Gans, 1999) that opens from the floor of the nasal chamber via the apical foramen of the septomaxilla (Tra 053). The canal passes anteriorly for a short distance, then splits into separate dorsal and ventral passages before penetrating the premaxilla at the juncture of the nasal process and alveolar plate (Tra 031) (Figs. 4C, 7B); these then emerge as paired foramina on the dorsal and ventral surfaces of the premaxillary rostral process. The rostral canal likely transmitted cutaneous branches of the medial ethmoidal nerve and a rostral branch of the maxillary artery (Oelrich, 1956). The large diameter of these passages (Tra 026) (Fig. 7D) suggests that both surfaces of the rostral process of the premaxilla were vascularized and innervated to an unusual degree as compared to other amphisbaenians. A region of relatively high tactile acuity in this area was evidently present in *Rhineura hatcherii*.

A pair of dental canals can be seen to penetrate ventromedially into the premaxilla from the floor of the rostral canals (Tra 033). The dental canals merge into a central median premaxillary canal (Tra 036) that extends for a short distance along the premaxillary septum, then splits into three separate dental canals (Tra 039), each supplying a premaxillary tooth locus.

Septomaxilla (Fig. 8; Tra 035–114). The septomaxilla is a paired element in *Rhineura hatcherii* that lies entirely within the narial cupola, where it contacts the premaxilla, maxilla, vomer, and nasal. In transverse section (Tra 067) it is an L-shaped bone, comprising a vertical lamina that contributes to the internasal septum and internarial girder and a horizontal lamina that spreads to form the roof of the vomeronasal chamber and a partial floor to the nasal chamber. The vertical lamina is tallest posteriorly, where it closely approaches its counterpart along the sagittal plane to form a composite internasal septum. A cartilaginous nasal septum filled the narrow median space that separates the right and left vertical laminae along the midline (Fig. 3A).

The vertical lamina narrows anteriorly to a sharp rostral spine that projects to roughly the middle of the nasal cavity (Tra 035), thus contributing to the

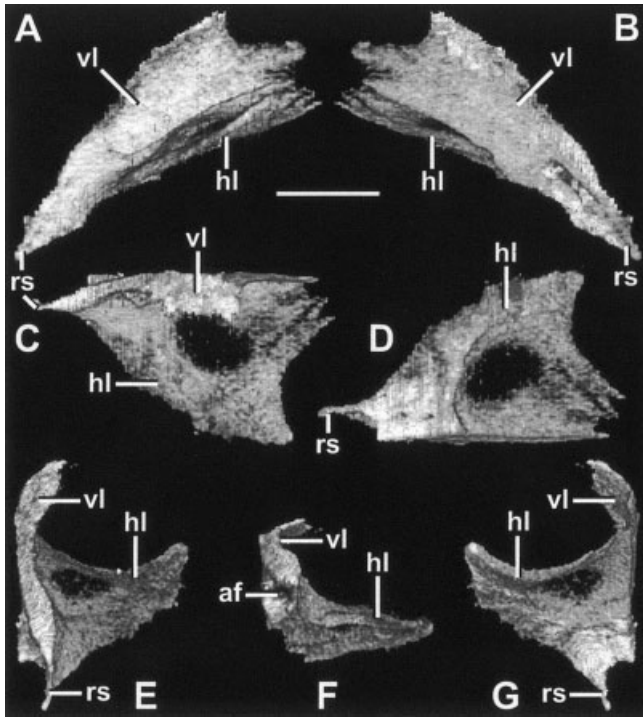


Fig. 8. Right septomaxilla (inverted) in (A) lateral, (B) medial, (C) dorsal, (D) ventral, (E) anterior, (F) oblique anterior, and (G) posterior views. Scale bar = 1 mm. af, apical foramen; hl, horizontal lamina; rs, rostral spine; vl, vertical lamina.

medial wall of the narial cupola and the internarial girder. The rostral spine also forms the lateral wall of the short ethmoid passageway (Tra 040) (Fig. 5C), a median longitudinal channel running from the nasal chamber to the surface of the face. Its nasal opening is the apical foramen, from which it runs for a short distance along the internarial girder (Tra 036–051) before branching into the premaxillary dorsal and ventral rostral canals and dental canals. The septomaxilla forms the lateral wall of the ethmoid passageway while the nasal forms its roof and the premaxilla its floor. Based in part on comparison with *Ctenosaura* (Oelrich, 1956), it probably conveyed trigeminal, premaxillary, and ethmoid branches of the ophthalmic nerve to the premaxillary dentition and cutaneous tissues of the rostrum.

The septomaxillary vertical lamina bends sharply at its base, where it spreads laterally onto the floor of the nasal passage as the horizontal lamina. It forms a thin, vaulted sheet of bone that bulges over the vomeronasal chamber (Fig. 4B) reflecting the large size of Jacobson's organ. In this region the horizontal lamina lies dorsal to the horizontal wing of the vomer and the palatal process of the maxilla (Fig. 3A).

Maxilla (Fig. 9; Tra 020–219). The paired maxilla in *Rhineura hatcherii* is roughly triangular in lateral view and L-shaped in transverse section. It makes contact with the premaxilla, septomaxilla,

vomer, palatine, ectopterygoid, nasal, prefrontal, and frontal. The facial process (=lateral plate of Montero and Gans, 1999) forms most of the lateral

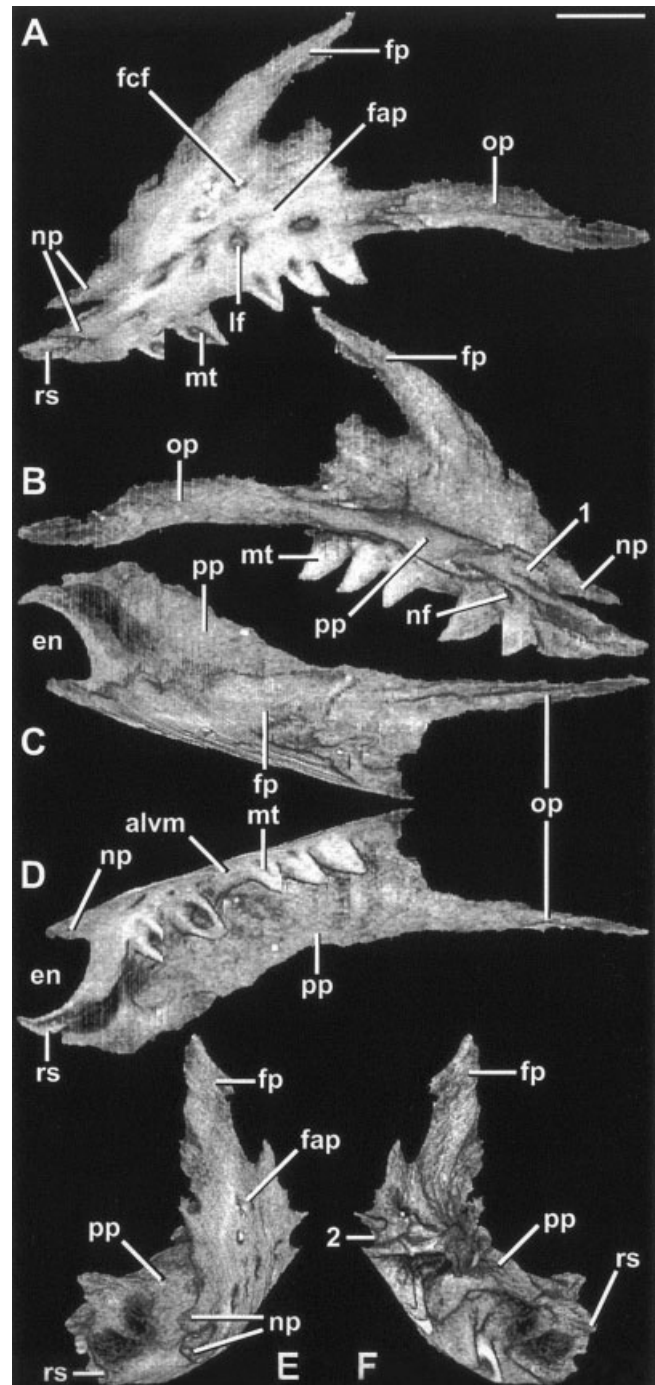


Fig. 9. Left maxilla in (A) lateral, (B) medial, (C) dorsal, (D) ventral, (E) anterior, and (F) posterior views. Scale bar = 1 mm. alvm, alveolar margin; en, external naris; fap, facial process; fcf, facial communicating foramen; fp, frontal process; lf, labial foramen; mt, maxillary tooth; nf, nutritive foramen; np, nasal process; op, orbital process; pp, palatal process; rs, rostral spine; 1, groove that receives rostral process of vomer; 2, groove for maxillary process of ectopterygoid.

surface of the facial segment of the skull, while the palatal process contributes primarily to the anterior palate. The two processes meet at an approximately right angle along the alveolar margin of the upper jaw, supporting six robust teeth. A short rostral spine projects anteromedially from the alveolar margin at one end of the maxilla, while an orbital process projects posteriorly from the other end of the palatal process beneath the orbit, where it contributes to the orbital floor.

The facial process expands over the side of the snout to contact the nasal anteriorly, the frontal dorsally, the prefrontal posteriorly, and the septomaxilla medially. Jutting from its superior edge is an elongate frontal process (Montero and Gans, 1999) that extends posterodorsally almost to the margin of the orbit, terminating in a point at the juncture of the frontal and prefrontal on the dorsal surface of the skull.

The maxillary canal runs longitudinally through the facial process of the maxilla just above the maxillary teeth (Tra 067–117) (Fig. 3B). The canal conveyed the superior alveolar nerve, a sensory branch of the maxillary branch of the trigeminal nerve (Oelrich, 1956). It entered the nasal chamber from the orbit and passed into the maxillary canal through the superior alveolar foramen (Tra 116) (Fig. 5B). As it courses through the facial process, the maxillary canal gives off four groups of subsidiary canals that supplied innervation to the teeth, surface of the snout, and inner surface of the nasal passage. Narrow dental canals penetrate the maxilla ventrally (e.g., Tra 083) (Fig. 5C), where they supplied a small nerve fiber to each maxillary tooth position. A linear series of large labial foramina exit the maxillary canal just above the bases of the maxillary teeth (Figs. 5C, 9A). Dorsal to these is a cluster of three additional communicating facial foramina that perforate the center of the facial process (e.g., Tra 077) (Fig. 5B). Collectively, these foramina conveyed cutaneous branches of the superior alveolar nerve and the maxillary artery (Oelrich, 1956) to the superficial tissues of the face. The canal exits into the narial cupola through the anterior inferior alveolar foramen (Tra 071) through which branches of the maxillary artery and superior alveolar nerve communicated to cutaneous tissues of the snout (Oelrich, 1956).

The nasal process projects from the anterolateral extremity of the maxilla, where it forks to clasp the lateral edge of the rostral process of the nasal (Tra 037); the notch within the fork extends into the maxilla to the level of the first maxillary tooth. The rostral spine of the maxilla forms the posterior rim of the naris and curves anteriorly, where it laterally grasps the alveolar plate of the premaxilla (Tra 030).

The palatal process of the maxilla (Fig. 9D) extends medially as a horizontal shelf whose anterior extremity contacts the vomer and forms a short floor beneath the nasal chamber. The maxillary palatal

process is overlapped anteriorly by the septomaxilla (Fig. 3A). It contacts the palatal process of the premaxilla anteroventrally (e.g., Tra 073) and the maxillary process of the palatine posterodorsally (Fig. 3C). A groove on the medial edge of the maxillary palatal process (Fig. 9B) receives the rostral process of the vomer (Figs. 3A, 5C). Behind this contact the maxillary palatal process also forms the lateral border of the fenestra vomeronasalis (Figs. 5C, 6C). Further posteriorly, behind the horizontal wing of the vomer, the maxillary palatal process forms the lateral margin of the choana. Incisive fossae on its palatal surface accommodate the tips of the dentary teeth (e.g., Tra 099).

The orbital process of the maxilla lies medial to the ectopterygoid for most of its length, enclosed between the ectopterygoid and the maxillary process of the palatine (Figs. 3D, 5B). At its posterior tip the orbital process meets the pterygoid, which separates it from the lateral edge of the palatine (Fig. 3F). As the orbital process passes beneath the orbital margin, it contacts the ectopterygoid in an interdigitating suture (Fig. 3C). The contribution of the maxilla to the orbital margin is small.

The angular junction of the facial and palatal processes of the maxilla marks its alveolar margin. Six tooth positions occupy the alveolar margin, the first lying near the base of the nasal process and the last lying just anterior to the orbit. Five subpleurodont teeth and one empty tooth position are present on the right maxilla, whereas six teeth are present on the left. The second tooth is the largest of the six. The teeth have bulbous, swollen bases that house large pulp cavities (Figs. 3A, 4A), and they are roughly circular in frontal cross section. The crowns are conical, unridged, and slightly recurved. Medial to the base of each tooth is a nutritive foramen (Figs. 4A, 9B). Nearly all of the maxillary teeth in this specimen sustained postmortem damage.

Nasal (Fig. 10; Tra 008–094). The nasal is a paired element. It is largely eroded away in both sides of this specimen (Fig. 6B), and the following description partly relies on other specimens of *Rhineura hatcherii* and on published accounts (Gilmore, 1928; Taylor, 1951; Estes, 1983). The nasal contacts the premaxilla, septomaxilla, maxilla, and frontal. It bears a sharp rostral process that joins the premaxillary rostral process to form the rostral blade of the snout (broken postmortem on left side of the specimen). The nasal rostral process is clasped by the nasal process of the maxilla lateral to the naris (e.g., Tra 037).

The nasal forms most of the anterior, dorsal, and lateral narial walls. A facial lamina arises laterally from the nasal to form much of the wall of the narial cupola. The facial lamina is a thin, gently convex sheet of bone closely applied against the medial surface of the facial process of the maxilla and the inferior surface of the frontal (e.g., Tra 073) (Fig. 4A). The superior surface of the facial lamina also

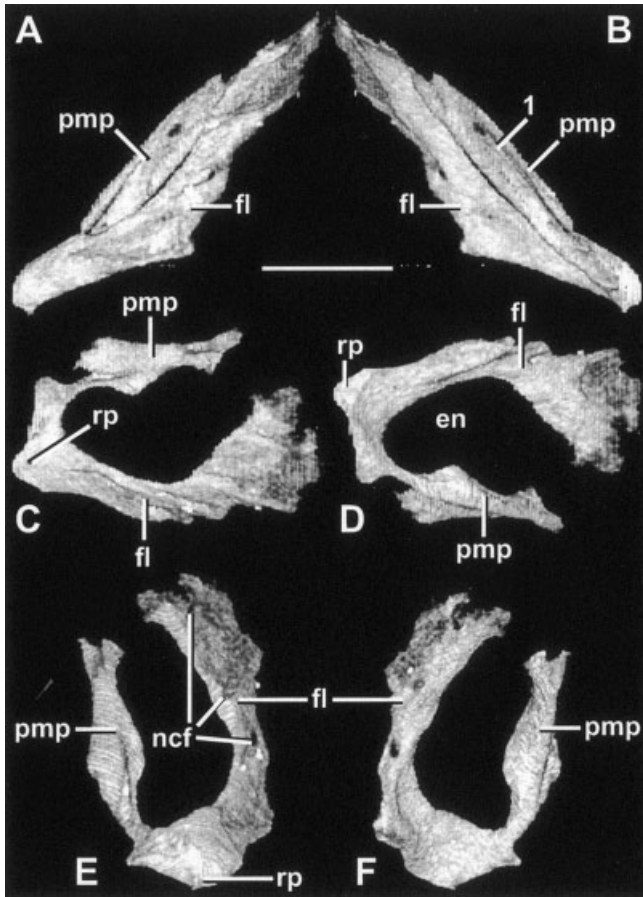


Fig. 10. Right nasal (inverted) in (A) lateral, (B) medial, (C) dorsal, (D) ventral, (E) anterior, and (F) posterior views. Scale bar = 1 mm. en, external naris; fl, facial lamina; ncf, nasal communicating foramen; pmp, premaxillary process; rp, rostral process; 1, groove that receives nasal process of premaxilla.

lies in close contact with the superior edge of the septomaxillary vertical lamina along the roof of the narial cupola. The facial lamina of the nasal is pierced by three communicating foramina (Figs. 3A, 9E). The ventralmost foramen forms an incisure on the posterior edge of the facial lamina, while the others penetrate where the bone is very thinned. All three foramina communicate between the nasal chamber and the external surface of the snout, and probably provided passage of cutaneous vasculature and innervation (see below). As indicated by a depression on the anterior margin of the dorsal plate of the frontal (Fig. 6B), the nasal ended posteriorly in a long superficial frontal lappet that overlapped the frontal and tapered to a point near the level of the orbit. The frontal lappet of the nasal is eroded away in this specimen.

The premaxillary process of the nasal extends posteriorly from the rostral process, approaching but not meeting the posterodorsal edge of the facial lamina. It abuts the dorsal edge of the rostral spine of the septomaxilla just posterior to the perforation of

the premaxilla by the rostral canal (Tra 042). The premaxillary process of the nasal grasps the dorsal edge of the nasal process of the premaxilla posteriorly (Figs. 4B, 5B) to the level of the septomaxillary apical foramen, and is gradually pinched out by the dorsal plate of the frontal (Tra 069).

Vomer (Fig. 11; Tra 040–199). The vomer is a paired element that contributes to the internarial girder, the floor of the vomeronasal chamber, the palate, and the borders of the choana. Between its anterior and posterior extremities, the dorsal surface of the vomer is slightly concave and its ventral surface is slightly convex. A rostral process (=anterior process of Montero and Gans, 1999) projects anteriorly, contacting the maxillary palatal process and the septomaxillary vertical lamina; its paired tips grasp the base of the premaxillary nasal process (Tra 048). The rostral process of the vomer is triangular in transverse section and forms a robust strut extending from near the posterior narial border to the posterior extremity of the vomeronasal chamber (Fig. 5C). The right and left rostral processes abut along a deep, flat median surface (Figs. 3A, 4C). The

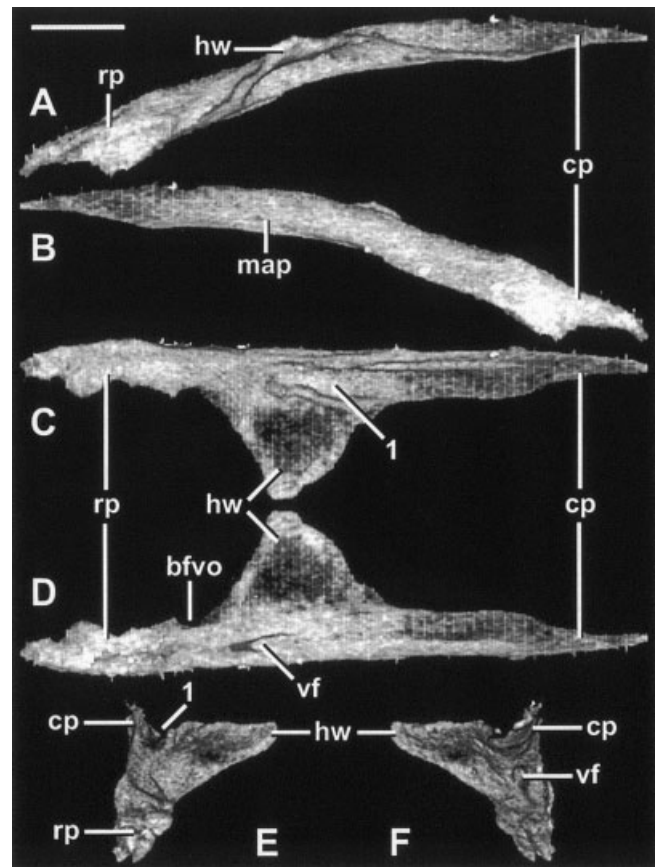


Fig. 11. Left vomer in (A) lateral, (B) medial, (C) dorsal, (D) ventral, (E) anterior, and (F) posterior views. Scale bar = 1 mm. bfvo, border of fenestra vomeronasalis; cp, choanal process; hw, horizontal wing; map, median articular plane; rp, rostral process; vf, vomerine foramen; 1, groove that receives vomerine process of palatine.

rostral processes form the core of a major structural element along the midline of the snout—they tie together projections of the premaxillae, septomaxillae, and maxillae into a complex internarial girder that braces the rostral blade, via the palate, against the basicranial axis. The rostral process abuts the palatal process of the maxilla, overlies the palatal process of the premaxilla, and underlies the horizontal lamina of the septomaxilla (e.g., Tra 072), forming the ventromedial border of the fenestra vomeronasalis.

Posterior to the rostral process, the vomer spreads laterally as a thin sheet of bone over the fenestra vomeronasalis and onto the palate, forming a horizontal wing (Montero and Gans, 1999) that contributes simultaneously to the palate and the floor of the nasal chamber for a short distance (Fig. 3B). The horizontal wing lies just anterior to the midpoint of the vomer (Fig. 11C) and its lateral extremity contacts and partially overlies the maxillary palatal process (Fig. 3B). A laterally diverging ridge along the dorsal surface of the horizontal wing reportedly marks the passage of the lacrimal duct in *Amphisbaena alba* (Montero and Gans, 1999). A comparable ridge may be seen on the horizontal wing in *Rhineura hatcherii* (Fig. 11C); however, the CT slices reveal that this ridge marks the edge of a groove that receives the vomerine process of the palatine (Tra 109–123) (Fig. 5B). A foramen pierces the vomer just posterior to the fenestra vomeronasalis (Figs. 3B, 11D), exiting dorsally just lateral to the groove holding the palatal vomerine process. This foramen transmitted branches of the anterior palatine nerve and inferior nasal artery (Oelrich, 1956).

The right and left vomers remain in contact along the midline via a flat surface (Figs. 3B, 11B) for approximately three-quarters of their length, until a small pyriform recess intervenes (Figs. 3C, 5B). The vomer gradually tapers posteriorly into a slender choanal process (=posterior process of Montero and Gans, 1999) that curves along the midline of the palate, terminating in a thin point wedged shallowly between the palatine, the cultriform process of the parabasisphenoid, and the vomerine process of the pterygoid (Fig. 3E).

Palatine (Fig. 12; Tra 100–238). The palatine is a paired element forming the roof of the palatal vault and portions of the floor and medial wall of the orbit. It extends posteriorly in an intricately interdigitating contact with the pterygoid. The right and left palatines are separated from each other by the choanal processes of the vomers, the parabasisphenoid, and a very narrow pyriform recess (Fig. 5B).

A vomerine process is formed by a slender anteromedial projection of the palatine that extends into a groove on the dorsal surface of the vomer, medial to the horizontal wing (Figs. 3B, 5B). A shorter maxillary process projects forward at the anterolateral extremity of the palatine (Fig. 3A) to loosely embrace the palatal process of the maxilla and the maxillary process of the ectopterygoid (Fig. 3C). The

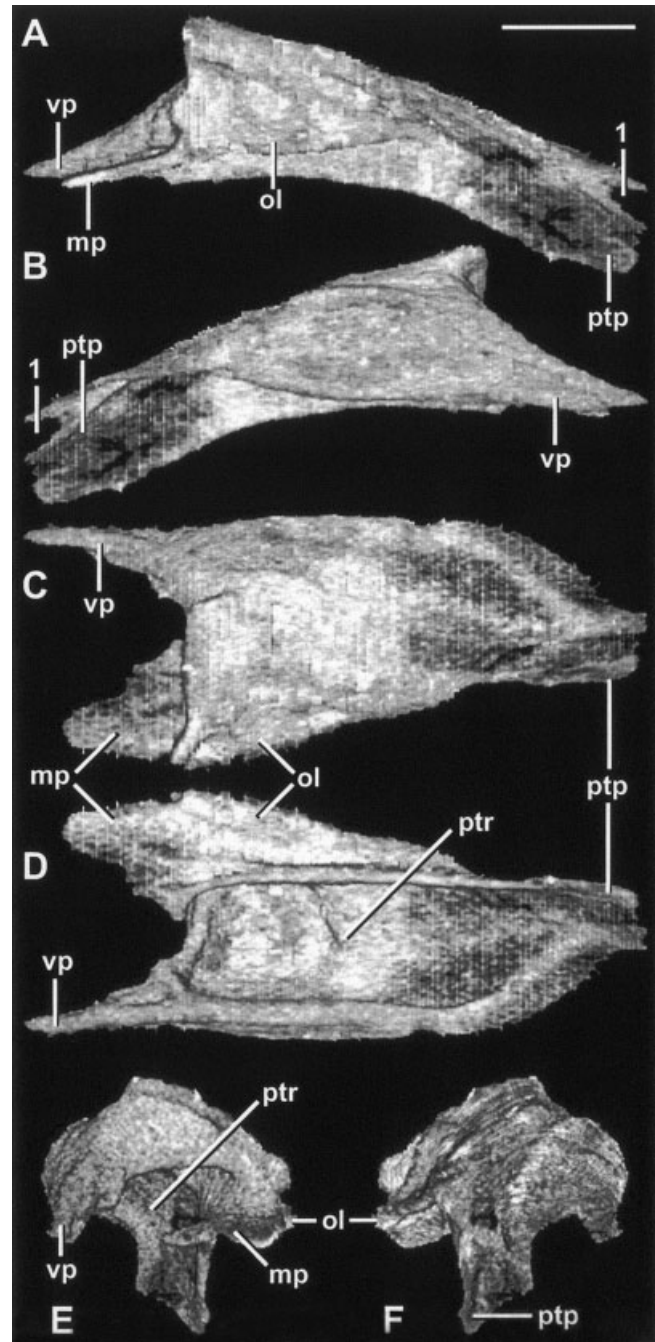


Fig. 12. Left palatine in (A) lateral, (B) medial, (C) dorsal, (D) ventral, (E) anterior, and (F) posterior views. Scale bar = 1 mm. mp, maxillary process; ol, orbital lamina; ptp, pterygoid process; ptr, palatal trough; vp, vomerine process; 1, groove that receives palatine process of pterygoid.

pterygoid process of the palatine projects posteriorly to clasp the vomerine process of the pterygoid and the orbital process of the maxilla (Fig. 3E), then makes a substantial contact with the pterygoid transverse process (Figs. 3F, 5C).

Above the roof of the choanal vault the superior surface of the palatine lies in close contact with the

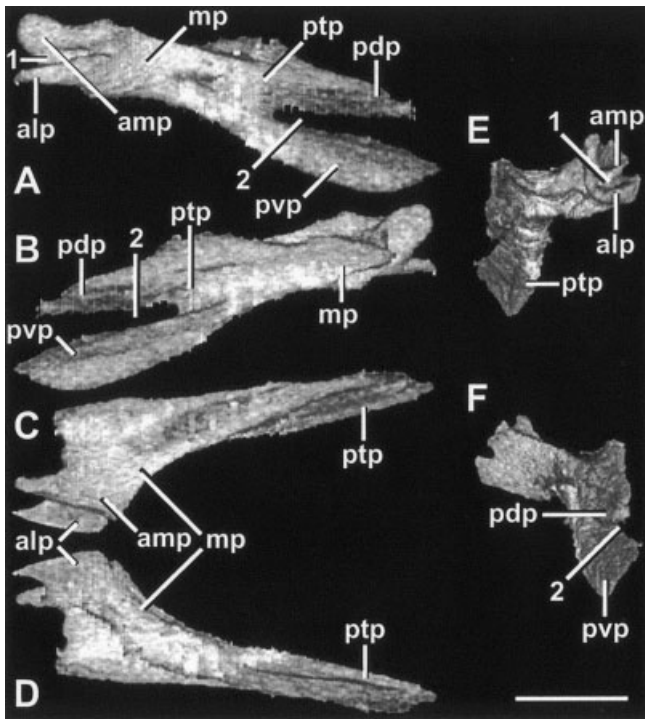


Fig. 13. Left ectopterygoid in (A) lateral, (B) medial, (C) dorsal, (D) ventral, (E) anterior, and (F) posterior views. Scale bar = 1 mm. alp, anterolateral process; amp, anteromedial process; mp, maxillary process; pdp, posterodorsal process; ptp, pterygoid process; pvp, posteroventral process; 1, groove that receives facial process of maxilla; 2, groove that receives orbital process of maxilla and transverse process of pterygoid.

frontal (Figs. 3C, 4A); as this surface arches laterally it becomes exposed in the orbital wall (Tra 141). Projecting ventrolaterally from its orbital face is a flange-like orbital lamina (Fig. 12D) that contacts the ectopterygoid along most of the length of the orbital floor (Tra 147–169). The palatine also contacts the prefrontal laterally (Fig. 3C) and the parabasisphenoid posteriorly (Figs. 3D, 4C).

The inferior surface of the palatine is smooth and arched along much of its length, forming a palatal trough that provides the bony roof of the choanal vault (Figs. 4B, 12D) and constitutes the posterodorsal border of the internal choana (Jollie, 1960). The trough is deepest anteriorly, becoming shallower posteriorly until the palatine eventually flattens out, ending in its contact with the pterygoid (Figs. 3F, 4B). In living amphisbaenians, the palatal trough is closed ventrally by soft tissues.

Ectopterygoid (Fig. 13; Tra 125–230). The ectopterygoid is a paired lateral element that lies between the maxilla and pterygoid along the lateral edge of the palate, where it also contributes to the floor of the orbit. In *Rhineura hatcherii* the ectopterygoid contacts the maxilla along most of its length, meeting the pterygoid posteriorly and the palatine and prefrontal medially.

The body of the ectopterygoid is short and thick, with a weakly forked maxillary process that extends anteriorly to clasp the facial process of the maxilla between separate anterolateral and anteromedial processes (Tra 131) (Figs. 5B, 13A). A strongly forked pterygoid process extends posteriorly along the orbital process of the maxilla as separate posterodorsal and posteroventral processes that form a tongue-and-groove suture with the orbital process of the maxilla and the transverse process of the pterygoid (Figs. 3E, 4A, 13A). The maxillary process lies in the frontal plane while the pterygoid process lies in the sagittal plane in the articulated skull. The ectopterygoid is exposed ventrally as a splint-like element lying lateral to the orbital process of the maxilla and medial to the transverse process of the pterygoid (Fig. 6C).

Pterygoid (Fig. 14; Tra 170–302). The pterygoid is a paired element lying on either side of the midline of the ventral surface of the skull. In *Rhineura hatcherii* it articulates with the maxilla, palatine and ectopterygoid anteriorly, and with the parabasisphenoid and quadrate posteriorly. The pterygoids form the posteriormost portion of the palate, and each pterygoid is elongate and slightly concave dorsoventrally.

The vomerine process (=anteromedial process of Montero and Gans, 1999) of the pterygoid (Fig. 14C) tapers to a thin point as it extends anteriorly and contacts the choanal process of the vomer (Fig. 3E). Among amphisbaenians, this pterygoid-vomer contact occurs only in some “shovel-headed” forms (Kearney, 2003). The vomerine process broadens posteriorly into a sheet that is closely applied against the inferior surface of the palatine in the medial wall of the palatal vault (Fig. 3F).

The transverse process of the pterygoid (Fig. 14C) contacts the ectopterygoid, maxilla, and palatine (Fig. 3E). This process exhibits three distinct anteriorly projecting fingers (Fig. 14C): the most lateral and prominent inserts into a notch on the lateral surface of the ectopterygoid (Tra 183) (Fig. 4A); the next most lateral fits between the ectopterygoid and the orbital process of the maxilla (Tra 188); and the third (most medial) inserts between the orbital process of the maxilla and the maxillary process of the palatine (Tra 193). Because the transverse process is wedged between the ectopterygoid and palatine (Fig. 6D), there is no suborbital fenestra.

Posteriorly, the quadrate process of the pterygoid (Fig. 14C) lies in tight contact with the parabasisphenoid as it extends posterolaterally, broadening to form a floor beneath the cavum epiptericum (Fig. 14C), an extracranial space that houses the Gasserian ganglion of the trigeminal nerve (Oelrich, 1956). The quadrate process curves dorsolaterally from its point of contact with the basiptyergoid process (Tra 279–300) (Fig. 3G) to grasp the quadrate. The quadrate process loosely contacts the basiptyergoid process via an

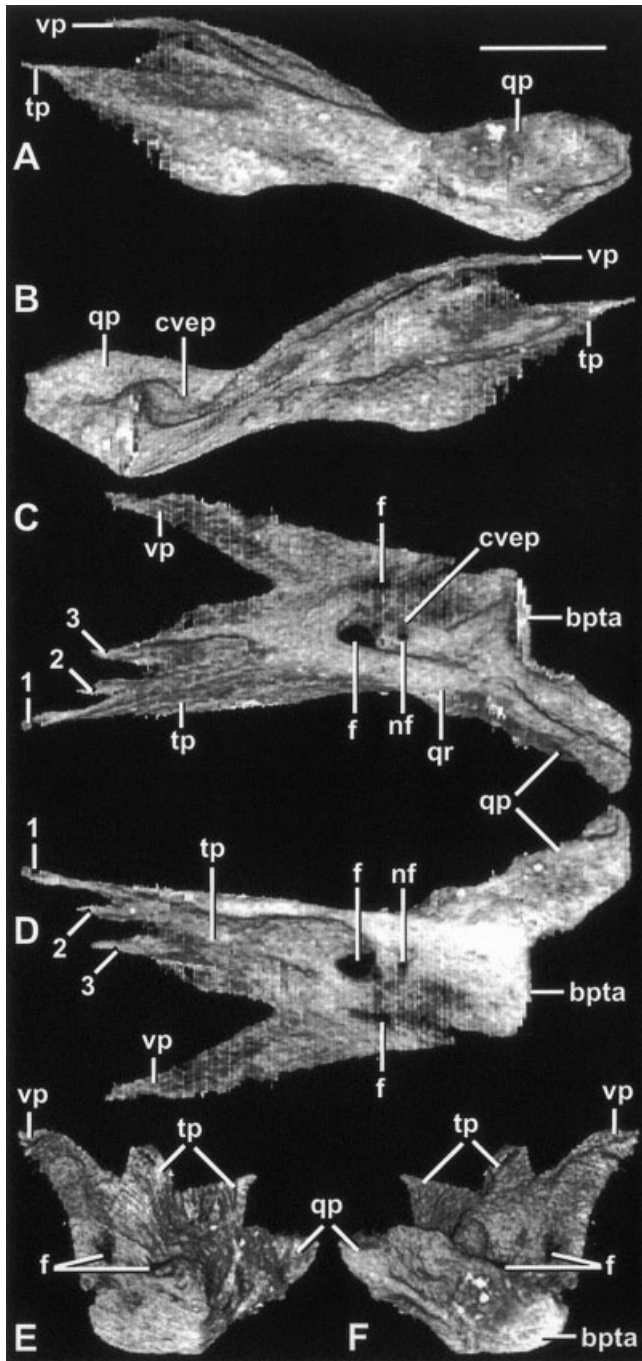


Fig. 14. Left pterygoid in (A) lateral, (B) medial, (C) dorsal, (D) ventral, (E) anterior, and (F) posterior views. Scale bar = 1 mm. bpta, basiptyergoid articular facet; cvep, cavum epiptericum; f, foramen; nf, nutritive foramen; qp, quadrate process; qr, quadrate ridge; tp, transverse process; vp, vomerine process; 1, inserts into lateral surface of ectopterygoid; 2, inserts between ectopterygoid and orbital process of maxilla; 3, inserts between orbital process of maxilla and maxillary process of palatine.

oblong cup-shaped articular surface (Tra 274–281) (Figs. 4A, 14F). The quadrate process also closely approaches the compound bone of the mandible (Tra 261–282) (Fig. 5C).

The pterygoid quadrate process forms the floor of the cavum epiptericum (Fig. 14C), where it is penetrated by two foramina. The larger, more anterior foramen lies slightly posterior to the midpoint of the bone, ventral to the quadrate ridge that runs from the transverse process posteriorly through the quadrate process. It probably transmitted the trigeminal mandibular nerve (V_3) to the adductor musculature, and may have carried an arterial branch as well. The smaller foramen, positioned posteromedial to the larger one, may also have carried a smaller branch of the mandibular nerve (V_3). Traveling anteriorly over the floor of the cavum epiptericum were main trunks of the ophthalmic (V_1), maxillary (V_2), and palatine branches of the facial nerve (VII) (Lakjer, 1927). Posterior to the larger foramen, the pterygoid is pierced dorsally and ventrally by small nutritive foramina (Fig. 14C,D). These immediately merge (Tra 255), then split into several canals (Tra 270) that traverse the quadrate process.

Jugal (Tra 126–147). A small jugal, visible only in the CT imagery (Fig. 3C), is present on the right side of the specimen. On the left side, matrix invades the corresponding space, suggesting that the left jugal fell away postmortem. The jugal is contacted by the facial process of the maxilla laterally and the maxillary process of the ectopterygoid medially. It is eroded at its dorsal tip; thus it is unknown whether the jugal played any role in forming a partial postorbital arch.

Prefrontal (Fig. 15; Tra 088–128). The prefrontal is a paired element in *Rhineura hatcherii* that contributes to the lateral surface of the snout, the anterior and dorsal walls of the orbit, and the anterodorsal orbital rim. The triradiate prefrontal comprises an antorbital process, a palatine process (=posterior face + ventrolateral process of Montero and Gans, 1999), and a postorbital process (=posteromedial process of Montero and Gans, 1999) that converge into a medially concave body referred to as the orbital plate. The prefrontal lies posterodorsal to the maxilla and ventrolateral to the frontal, contacting the maxilla laterally, ventrally and dorsally, the frontal dorsomedially, and the palatine and ectopterygoid posteroventrally.

The antorbital process of the prefrontal extends anteriorly from the orbit as a thin sheet of bone (Fig. 15A) that lies closely applied against the medial surfaces of the maxillary facial and frontal processes (Figs. 3B, 5A); thus it is largely hidden from external view (Fig. 6A). It narrows and gradually terminates anteriorly, at a level between the third and fourth maxillary teeth (Tra 089). The lacrimal foramen does not pierce the prefrontal, but rather enters between the prefrontal and maxilla at the junction of the antorbital and palatine processes and the orbital plate (Tra 125). The lacrimal foramen marks the passage of the lacrimal duct from the orbit into the nasal chamber. It is a large opening, suggesting that a large gland filled much of the orbit.

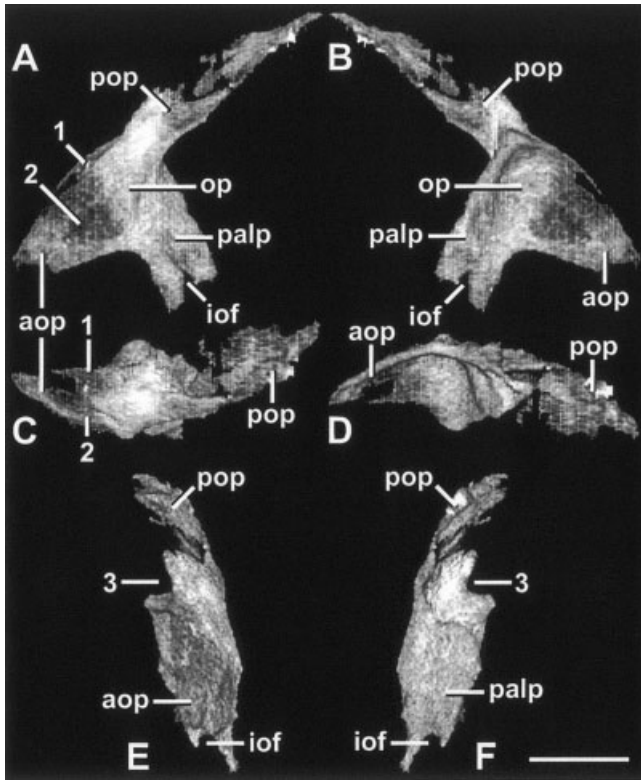


Fig. 15. Left prefrontal in (A) lateral, (B) medial, (C) dorsal, (D) ventral, (E) anterior, and (F) posterior views. Scale bar = 1 mm. aop, antorbital process; iof, infraorbital foramen; op, orbital plate; palp, palatine process; pop, postorbital process; 1, area of overlap by frontal process of maxilla; 2, area of overlap by facial process of maxilla; 3, groove that receives lateral edge of dorsal plate of frontal.

The palatine process of the prefrontal forms a smooth, concave sheet that projects ventromedially to form the anterior wall of the orbit (Fig. 6A). It is closely applied against the superior surface of the palatine (Fig. 3C). Distally it forms a notch that, together with the maxillary process of the palatine and the palatal process of the maxilla, marks the infraorbital foramen (Tra 135). As it arches over the infraorbital foramen the palatine process continues its contact with the dorsal surface of the palatine medial to the foramen, while lateral to the foramen its distal tip inserts between the palatal process of the maxilla and the maxillary process of the ectopterygoid (Fig. 5B). Thus, the infraorbital foramen is encircled by the prefrontal, maxilla, ectopterygoid, and palatine bones. The infraorbital foramen provided passage for the infraorbital nerve from the floor of the orbit into the nasal chamber (Tra 133), to become the superior alveolar nerve (Oelrich, 1956). A comparable notch in *Amphisbaena alba* (Montero and Gans, 1999) was misidentified as a groove for the passage of the lacrimal duct.

The postorbital process of the prefrontal projects posterodorsally. It contacts the supraorbital process of the frontal (Figs. 3C, 4A) and, more posteriorly,

the anterolateral process of the parietal which extends along the lateral edge of the frontal. At this point of contact (Tra 162), both the postorbital process of the prefrontal and the anterolateral process of the parietal are clasped by the supraorbital process of the frontal.

Frontal (Fig. 16; Tra 061–241). In *Rhineura hatcherii* the frontal is a paired element comprising two main divisions, the dorsal plate and the descending process, each with its own complex form and function. The superficial surface forms the leading surface or dorsal plate of the “shovel snout” (Fig. 6B). It contributes greatly to the shovel-headed appearance of the skull and its surface is heavily sculptured. Beneath the dorsal plate lies the descending process (Fig. 6A), which is an inclusive term for a latticework of distinct laminae involved in forming the deeply sunken orbit and a bony tube that completely encircles the forebrain.

The dorsal plate contacts the septomaxilla, maxilla, nasal, prefrontal, and parietal. It serves as a facial shield while also contributing to separate roofs over the nasal chamber and the cranial cavity (Figs. 3B,C, 4B). The dorsal plate broadly overhangs the orbit via a supraorbital process, creating a wide orbital roof and also contributing to the orbital rim (Fig. 4A). The dorsal plate is gently convex and inclined toward the rostrum, with its widest point immediately above the orbit.

The left and right frontals appear superficially to abut in a straight suture extending along the midline of the dorsal plate (Fig. 6B). However, the CT imagery shows that the frontals contact each other in a tongue-and-groove syndesmosis (Fig. 16B) over most of their length (Tra 077–112, Tra 142–169). The dorsal plate is partially overlain by a small frontal lappet of the nasal as indicated by a depression at the anterodorsal margin of the dorsal plate (Fig. 16C). The dorsal plate gradually narrows behind the orbit, terminating in a pointed parietal lappet that broadly overlies the parietal (Figs. 3E, 4B, 16C).

Superficially, the frontoparietal suture appears W-shaped and rather simple (Fig. 6B). However, the CT imagery reveals that each frontal interdigitates in a complex suture with the parietal (Figs. 3D, 4A) and that substantial portions of each frontal underlie the parietal (Fig. 16C). Deep notches in the posterior edge of the dorsal plate (Fig. 16F) receive anteriorly projecting fingers of the parietal in a three-dimensionally complex syndesmosis (Fig. 3D). The dorsal plate is also partially overlain by the frontal process of the maxilla (e.g., Tra 117) (Fig. 4A) and the postorbital process of the prefrontal (e.g., Tra 131), whose extents of overlap are marked by shallow ridges that can be seen on the isolated bone (Fig. 16C). The supraorbital process of the frontal holds the tip of the postorbital process of the prefrontal and the anterolateral process of the parietal just above the orbit (Figs. 3D, 16E).

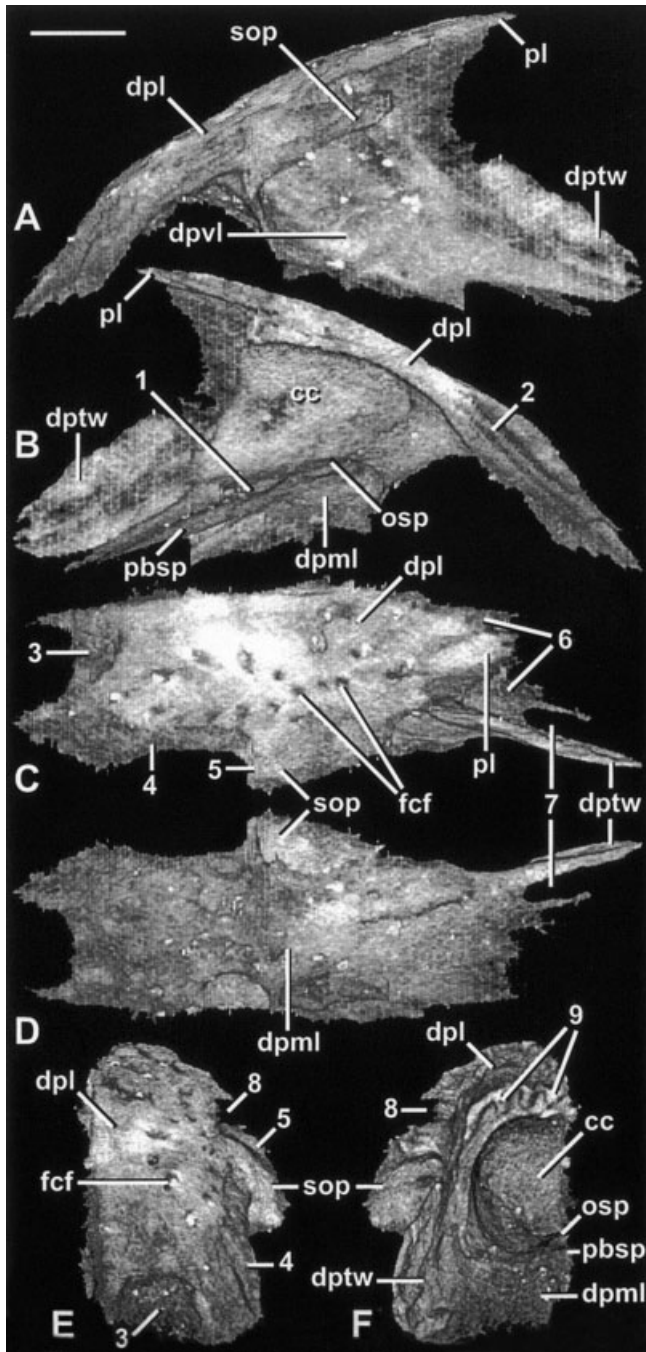


Fig. 16. Left frontal in (A) lateral, (B) medial, (C) dorsal, (D) ventral, (E) anterior, and (F) posterior views. Scale bar = 1 mm. cc, cranial cavity; dpl, dorsal plate; dpml, descending process medial lamina; dptw, descending process temporal wing; dpvl, descending process vertical lamina; fcf, frontal communicating foramen; osp, orbitosphenoid process of medial lamina; pbsp, parabasisphenoid process of medial lamina; pl, parietal lappet; sop, supraorbital process; 1, frontal-frontal contact (medial laminae of descending processes); 2, frontal-frontal contact (dorsal plates); 3, area of overlap by frontal lappet of nasal; 4, area of overlap by frontal process of maxilla; 5, area of overlap by post-orbital process of prefrontal; 6, area of overlap by parietal; 7, groove that receives postorbital process of prefrontal and anterolateral process of parietal; 8, notches that receive anteriorly projecting fingers of parietal.

The surface of the dorsal plate is extensively pitted and sculptured. The CT imagery reveals that the superficial channels actually penetrate the frontals (Fig. 3B,C) and communicate via an extensive system of canals and foramina (Fig. 4B) that presumably provided vascularization and/or tactile innervation to the snout. There appears to be both mediolateral and anteroposterior patterning in this array of channels. Along each frontal the communicating foramina are arrayed in three parasagittal rows (Fig. 16C) that open to the surface from a common longitudinal frontal canal (Fig. 3C). Feeding into the frontal canal was a branch of the trigeminal ophthalmic nerve that enters from the dorsomedial wall of the orbit (Tra 153). More anteriorly, another pair of tiny passages enters the frontal canal through the wall of the anterolateral cranial cavity (Tra 127), and the anterior tip of the frontal was probably penetrated by the trigeminal maxillary branch, which entered from the roof of the nasal chamber (Tra 086).

Beneath the dorsal plate is the complex descending process of the frontal (Fig. 16A). It contacts the prefrontal, palatine, orbitosphenoid, parabasisphenoid, parietal, and prootic region of the otic-occipital complex. The descending process is organized around a vertical lamina of bone that descends from the dorsal plate toward the floor of the orbit and braincase (Fig. 4A). Inferiorly, the vertical lamina bifurcates and broadens into two approximately horizontal laminae, one directed laterally and the other medially (Fig. 3C). An additional projection from the descending process of the frontal is the temporal wing (Fig. 16A), which projects posteriorly from the vertical lamina to form part of the lateral wall of the braincase.

The vertical lamina forms the medial wall of the orbit as it descends from beneath the dorsal plate, then it spreads as a curved sheet-like process beneath and in front of the eye, contributing to the floor and anterior wall of the orbit (Fig. 6A). Near its junction with the dorsal plate the vertical lamina is penetrated by the superior orbital foramen (Tra 148–149) that transmitted cutaneous innervation and vasculature to the posterior surface of the dorsal plate.

The vertical lamina also forms the long lateral wall of the anterior part of the cranial cavity (Tra 136–183) (Fig. 3C). The base of this wall curves inward as the medial lamina, which forms a floor beneath the cranial cavity as it projects to contact its counterpart along the ventral midline in a complex tongue-and-groove suture (Figs. 3C, 4C, 16B). Thus, the frontals form a complete and robust bony tube that encircles the forebrain, an unusual condition that is present throughout amphisbaenians (Zangerl, 1944; Vanzolini, 1951) and in some other squamates such as snakes. There appear to be no perforations in this structure, with the exception of the pair of tiny canals that pass into the frontal

canal through the lateral walls of the cranial cavity (Tra 127). Additionally, the cranial cavity is not closed anteriorly, where the olfactory fenestra provided a large passageway for the neuronal axons of the olfactory epithelium of the nasal chamber.

The medial lamina sends two processes medially as it projects beneath the forebrain (Tra 180) (Figs. 5A, 16B). Dorsally it sends a thin orbitosphenoid process that clasps the edge of the orbitosphenoid. Ventrally it sends a stout parabasisphenoid process that holds the edge of the parabasisphenoid, beginning at the level of the anterior edge of the parietal (Tra 165) and ending at the level of the apex of the coronoid process (Tra 200). This architecture is similar to that reported in the amphisbaenian *Monopeltis capensis* (see Kritzinger, 1946).

The descending process also contributes significantly to the wall of the braincase via a temporal wing (Tra 205–240). The temporal wing projects posteriorly over the alar process of the prootic and the temporal lamina of the parietal (Figs. 4A, 6A), where it provided a broad attachment surface for parts of the adductor and pterygoideus musculature. It forms a broad outer wall around the braincase, but is separated from the cranial cavity by intervening processes of the parietal and prootic (Fig. 3F; see below) which the temporal wing overlies in planar apposition. The temporal wing is weakly developed in most amphisbaenians, but in many “shovel-headed” forms (including *Rhineura*, *Leposternon*, *Dalophia*, and *Monopeltis*) it is well developed (Kearney, 2003). The temporal wing was misidentified as the orbitosphenoid in several fossil rhineurids (Berman, 1973, 1976). However, the CT data show that the orbitosphenoids are completely enclosed within the braincase by the frontal, parietal, and prootic (Fig. 3E; see below) such that they are hidden from external view.

Parietal (Fig. 17; Tra 138–350). The parietal is a single element in *Rhineura hatcherii*, but it may have developed from paired ossification centers that fused early in ontogeny, as in *Amphisbaena* (Montero et al., 1999). The parietal is azygous in all amphisbaenians and forms a saddle-shaped element that is constricted at the narrowest point of the skull, just behind the frontoparietal suture. The anterodorsal surface of the parietal contributes a small triangular process to the deflected facial segment of the skull. A midline sagittal crest arises just behind the point of deflection and extends posteriorly along the entire length of the bone. In this specimen the sagittal crest is broken to expose the tube that received the cartilaginous extension of the processus ascendens of the supraoccipital, giving the false appearance of a pineal foramen (Figs. 4A, 6B). As in other amphisbaenians, there is no pineal foramen. The parietal forms most of the roof and dorsolateral walls of the cranial cavity, and its ventral surface is smooth.

Anterodorsally the parietal contacts the frontal in a complex interdigitating suture (Figs. 4A, 6B). At the point of deflection between the facial and cranial segments of the skull, the apical process of the parietal (Fig. 17B) forms the tallest prominence of the skull as it projects anterodorsally between the frontals. The anterior edge of the parietal projects forward as several unexposed fingers that insert into notches in the posterior margin of the dorsal plate of the frontal (Fig. 3D). Adjacent to these is the anterolateral process (Fig. 17B) that overlaps the frontal (Figs. 3E, 4A). The temporal lamina of the parietal (Fig. 17B) descends ventrolaterally from the skull roof. It projects forward over much of the cranial cavity to contact the postorbital process of the prefrontal at a point where both are grasped by the supraorbital process of the frontal (Fig. 3D). The temporal lamina is overlapped laterally by the temporal wing of the frontal (Figs. 3F, 4A), which leaves a ridge on the isolated parietal (Fig. 17A). Its inferior surface contacts the alar process of the prootic (Fig. 3F), thereby completely enclosing the braincase and excluding the temporal wing of the descending process of the frontal from participation in the endocranial wall. Anteriorly the alar process clasps the temporal lamina of the parietal (e.g., Tra 227), but posteriorly this reverses and the temporal lamina clasps the alar process (e.g., Tra 241).

The parietal broadly overlies the ossified roof of the vestibular chamber of the otic capsule (see below) via a pair of otic–occipital lappets (Tra 302–343) (Fig. 17B). There is no posttemporal fenestra and no supratemporal process of the parietal. A notch on the posteroventral margin of the parietal (Fig. 17E) receives the cartilaginous extension of the supraoccipital ascending process. The junction of the parietal and the ascending process of the supraoccipital is secured by two small descending fingers of the parietal (Figs. 3I, 17E) that insert into corresponding notches on the dorsal surface of the supraoccipital.

Squamosal (Figs. 3H, 6A; Tra 302–330). The squamosal is a paired element that is only vestigially present in *Rhineura hatcherii*. Its margins are difficult to discern except where it has a broad articulation with the quadrate. It forms a pyramidal, rugose mass that grasps the anterolateral edge of the paroccipital process of the otic capsule (Figs. 3H, 5B) and is fused to this process over part of its length. Posteriorly it can be discerned in the CT sections as a relatively spongy mass of peripheral bone, but anteriorly its fusion with the otic capsule is evident. The squamosal provides the primary articulation of the stout quadrate with the cranium. The quadrate also abuts the otic capsule ventromedial to the squamosal (e.g., Tra 309). The quadrate–squamosal joint lies on the ventrolateral face of the otic capsule, and the large jugular recess opens posterolateral to the squamosal.

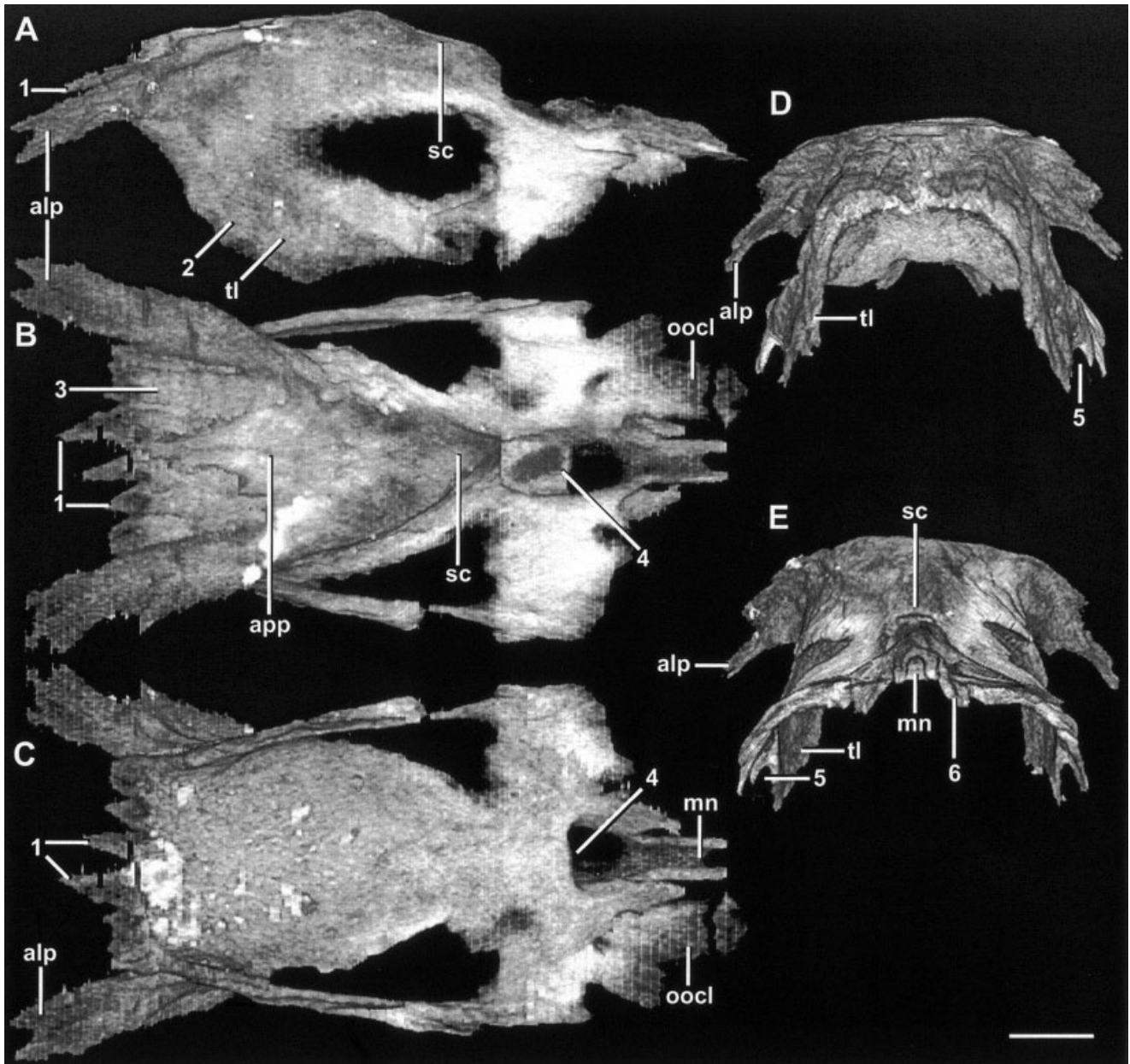


Fig. 17. Parietal in (A) lateral, (B) dorsal, (C) ventral, (D) anterior, and (E) posterior views. Anterior to left in A–C. Scale bar = 1 mm. alp, anterolateral process; app, apical process; mn, medial notch; oocl, otic-occipital lappet; sc, sagittal crest; tl, temporal lamina; 1, insert into notches on posterior margin of dorsal plate of frontal; 2, area of overlap by temporal wing of descending process of frontal and alar process of prootic; 3, area of overlap by parietal lappet of frontal; 4, tube that receives cartilaginous process ascends of supraoccipital; 5, groove for alar process of prootic; 6, inserts into notch on dorsal surface of supraoccipital.

Otic-occipital complex (Figs. 3, 18; Tra 139–411). In *Rhineura hatcherii*, as in amphisbaenians generally (Zangerl, 1944; Montero and Gans, 1999), many elements of the ear, braincase, basicranium, and occiput that remain as separate bones for at least part of postnatal ontogeny in other squamates are completely co-ossified. The separate embryonic ossifications of the otic and occipital units become conjoined above and below the foramen magnum, creating the fused otic-occipital complex. This com-

plex is figured and described as a single unit below. For convenience in more general comparisons among squamates, the constituent parts are then described region-by-region and, where possible, by comparison to the elements as they are known in *Amphisbaena* (Montero and Gans 1999; Montero et al., 1999). Finally, we summarize the internal morphology of the endocranium and otic capsule from anterior to posterior as viewed in successive transverse slices (Fig. 3).

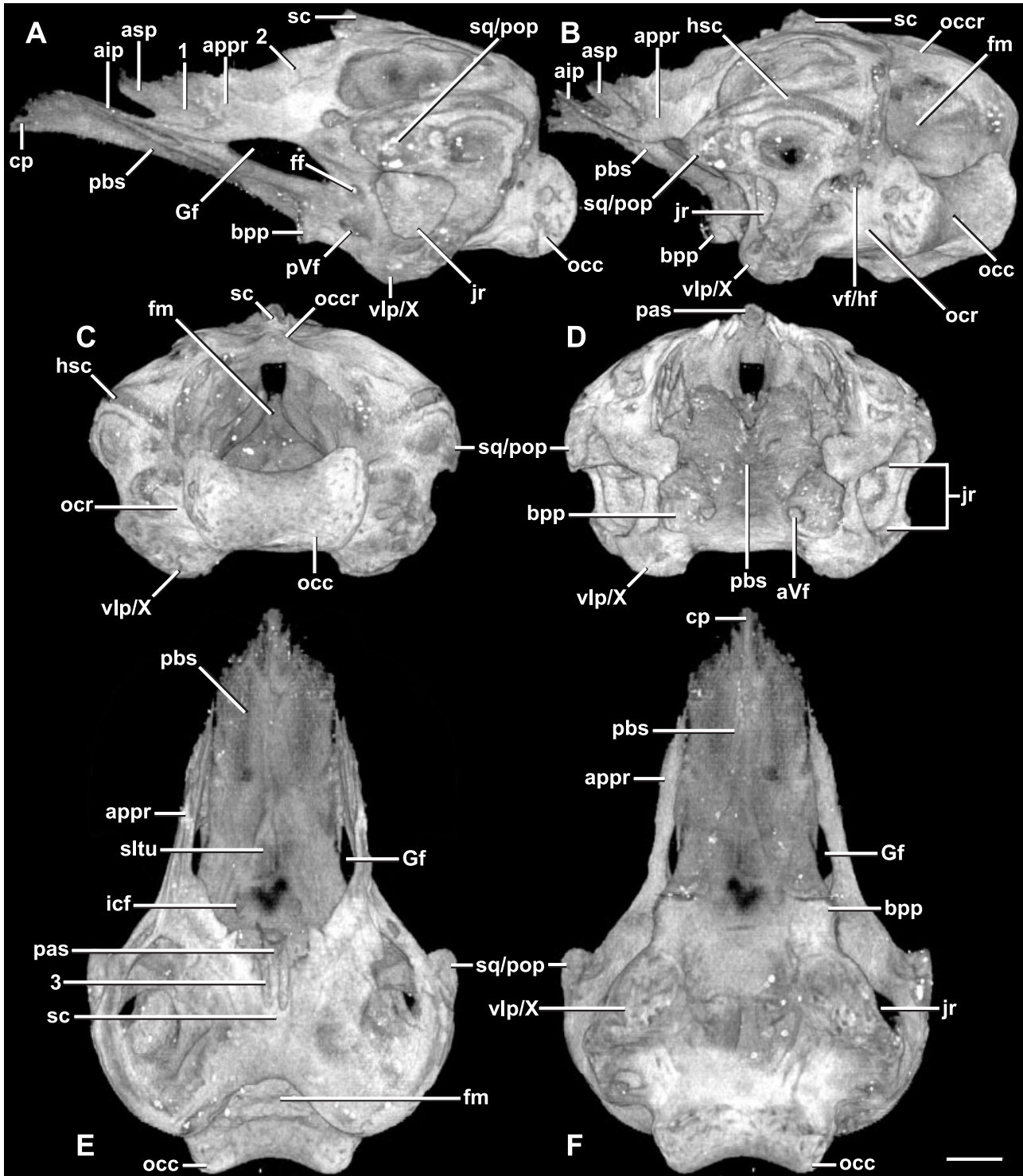


Fig. 18. Otic-occipital complex in (A) lateral, (B) oblique lateral, (C) posterior, (D) anterior, (E) dorsal, and (F) ventral views. Anterior to left in A-B, anterior up in E-F. Scale bar = 1 mm. aip, anterior inferior process of alar process of prootic; appr, alar process of prootic; asp, anterior superior process of alar process of prootic; aVf, anterior Vidian foramen; bpp, basiptyergoid process; cp, cultriform process of parabasisphenoid; ff, facial foramen; fm, foramen magnum; Gf, Gasserian foramen; hf, hypoglossal foramen; hsc, horizontal semicircular canal; icf, internal carotid foramen; jr, jugular recess; occ, occipital condyle; ocr, occipital crest; ocr, occipital recess; pas, processus ascendens of supraoccipital; pbs, parabasisphenoid; pop, paroccipital process; pVf, posterior Vidian foramen; sc, sagittal crest; sltu, sella turcica; sq, squamosal; vf, vagus foramen; vlp, ventrolateral process; X, "Element X"; 1, area of overlap by temporal wing of descending process of frontal; 2, area of overlap by temporal lamina of parietal; 3, groove that receives descending finger of parietal.

External anatomy of otic–occipital complex (Fig. 18). Viewed from the side (Fig. 18A) the otic–occipital complex inclines from its shallowest anterior point at the cultriform process tip (Fro 092) to its deepest posterior point (Fro 164) where the “Element X” (Zangerl, 1944) ventrally caps the ventrolateral process. The parabasisphenoid forms the anteriormost and median portions of the basicranium, while the cranial cavity is bounded laterally by the otic complex and dorsally and posteriorly by the occipital complex.

In anterior view (Fig. 18D) the otic–occipital complex is roughly oval. Its dorsal surface rises to an apex that is formed by the processus ascendens of the supraoccipital. The widest point occurs at the level of maximum lateral inflection of the horizontal semicircular canal within the osseous paroccipital process. Although open at the olfactory fenestra, the cranial cavity is mostly obscured from view by the dorsally inclined parabasisphenoid and the alar processes of the prootics. At the medial corner of the basiptyergoid process lies the anterior Vidian foramen (Tra 280). The jugular recess is largely visible in this view owing to its anterolateral orientation.

In dorsal view (Fig. 18E) only the posterior half of the otic–occipital complex has a dorsal roof. The parabasisphenoid floor of the cranial cavity is exposed anteriorly, and the cavum epiptericum is visible through the Gasserian foramen. Just behind the sella turcica, the alar processes of the prootics converge dorsally to form the beginnings of the endocranial roof. The otic–occipital complex is roofed posteriorly by the supraoccipital, which is incised by an inverted U-shaped notch along the dorsal border of the foramen magnum. Along the dorsal midline of the supraoccipital projects a sagittal crest (which is continued forward in the articulated specimen as the sagittal crest of the parietal) and along its posterodorsal margin is a small occipital crest. The processus ascendens of the supraoccipital, which extends from the anterior end of the sagittal crest, fits into a median notch on the parietal. On either side of the processus ascendens is a longitudinal groove that receives a descending finger of the parietal (Figs. 3I, 18E). The otic capsules are smooth and bulbous and form much of the dorsal surface of the otic–occipital complex. From the back of the otic–occipital complex protrudes the occipital condyle.

In ventral view (Fig. 18F) the otic–occipital complex is roughly triangular, with the anterior tip of the cultriform process forming the apex of the triangle and the otic capsules forming its corners. The alar process of the prootic extends anteriorly along the margin of the parabasisphenoid, arching above the Gasserian foramen which is visible between these two elements. The basiptyergoid process lies just posterior to the alar process, its anterior and lateral margins forming almost a right angle. Further posteriorly lies the ventrolateral process capped by “Element X.” The voluminous otic capsules lie

behind the basiptyergoid processes, and closing the cranial cavity posteriorly is the occipital arch and huge occipital condyle.

Parabasisphenoid complex. In *Rhineura hatcherii* the parasphenoid and basisphenoid are co-ossified to form the parabasisphenoid, which in turn is partially co-ossified with the basioccipital. Thus, the boundaries between these elements can only be estimated. The cultriform process extends over approximately the anterior half of the otic–occipital complex. The basiptyergoid process lies midway between the tip of the cultriform process and the occipital condyle, and midway between these two articulations lies the protuberant, rugose ventrolateral process (Fig. 18F). The cultriform process of the parabasisphenoid inserts into the median space formed between the choanal processes of the vomers, the palatines, and the medial laminae of the descending processes of the frontals (Figs. 3C, 5B). The parabasisphenoid then broadens (Fig. 18F), forming a horizontal plate that separates the palatine from the medial lamina of the descending process of the frontal (Fig. 3E). The parabasisphenoid lies against the dorsal surface of the pterygoid (e.g., Tra 231) and the two elements lie in contact as they extend posteriorly to a point where the wide, rectangular basiptyergoid process projects into its articulation with the pterygoid (Tra 279) (Fig. 6C).

The anterior floor of the cranial cavity is formed by the superior surface of the parabasisphenoid (Fig. 18E). The sella turcica forms a shallow basin in the floor of the parabasisphenoid, just above the basiptyergoid process, where it held the pituitary gland. The internal carotid foramen opens into the cranial cavity through the floor of the sella turcica (Figs. 3G, 18E).

The parabasisphenoid is penetrated by the posterior Vidian foramen (Fig. 18A), which opens into the Vidian canal between the basiptyergoid process and the jugular recess (Fig. 3H). The canal conveyed the internal carotid artery and palatine branch of the facial nerve (VII) longitudinally through the parabasisphenoid until opening anteroventrally beneath the sella turcica (deBeer, 1937; Oelrich, 1956; Jollie, 1960). The canal continues its anterior course through the parabasisphenoid and emerges through the anterior Vidian foramen (Tra 277) (Fig. 18D) into the cavum epiptericum.

The basiptyergoid process protrudes sharply beneath the Gasserian foramen. It presents a vertical articular surface (Figs. 4A, 18A) whose geometry suggests it was probably a synovial joint. The ventrolateral process swells ventrally behind the basiptyergoid process (Figs. 4A, 18F). The ventrolateral process is capped by “Element X” (Zangerl, 1944), the homology of which is problematic. Interpretations range from a sphenoccipital epiphysis (Lakjer, 1927; Jollie, 1960; Gans, 1960, 1978) to a neomorph (therefore “X elements” of Zangerl, 1944) to a basitemporal element (Vanzolini, 1951) to a

prootic element (Kesteven, 1957). In this specimen of *Rhineura hatcherii*, "Element X" is fused to the ventrolateral process, although sutural remnants are still barely discernable. Its surface is rugose and its internal structure is spongy.

Otic complex. The embryonic otic capsule, which in other squamates ossifies as separate prootic and opisthotic bones, co-ossifies in amphisbaenians along with the rudimentary squamosal (when present) and "Element X" to form a single fused otic complex (Zangerl, 1944; Kesteven, 1957; Montero et al., 1999). The quadrate and stapes both have synovial articulations with the otic complex.

The otic complex is conjoined to the occipital complex above and below the foramen magnum (Fig. 18C). The supraoccipital forms the roof of the cranial cavity and dorsally unites the right and left otic capsules. The exoccipital is confluent with the posteroventral wall of the otic capsule ventrolateral to the foramen magnum, where it encloses the occipital recess and vagus and hypoglossal foramina (Fig. 18B).

In rhineurid amphisbaenians the alar process of the prootic (Figs. 4A, 5A, 6A, 18A) is extremely well developed and extends anteriorly to contact the temporal wing of the frontal. Zangerl (1944) considered the alar process to be a separate pleurosphenoid based on his observation of a discrete ossification center in *Leposternon*.

However, Rieppel (1981) found no suture between this process and the prootic, and therefore suggested that it might be the alar process of the prootic, as seen in other lizards. Montero and Gans (1999) reported that this process in *Amphisbaena alba* is a cartilage replacement element rather than a membranous ossification, as in other fossorial lizards, and argued that it therefore cannot be homologous to the alar process of the prootic. Thus, the alar process of the prootic in amphisbaenians may represent the membranous extension of a more generally distributed element preformed in cartilage, composed of a material known as appositional bone or *Zuwachsknochen* (Patterson, 1977; Starck, 1979).

The alar process of the prootic contributes to the lateral closure of the braincase. It is overlapped anteriorly by the temporal wing of the frontal and dorsally by the temporal lamina of the parietal (Figs. 3F, 4A, 6A), whose facets of overlap form ridges on its surface (Fig. 18A). In *Rhineura hatcherii* the alar process is well developed and forked into anterior superior and anterior inferior processes. The inferior process articulates with the edge of the parabasisphenoid ventral to the base of the vertical lamina of the frontal (Fig. 3E). The anterior superior process lies dorsomedial to the descending process of the frontal, lateral to the orbitosphenoid, and ventral to the temporal lamina of the parietal (Fig. 3E).

The alar process of the prootic divides posteriorly into superior and inferior rami as it bifurcates

around the large Gasserian (trigeminal) foramen (Tra 246) (Fig. 18A). The parabasisphenoid lies in medial contact with the inferior ramus until the latter ends (Tra 257), at which point the parabasisphenoid forms the ventral rim of the Gasserian foramen. The combined root of the trigeminal nerve (V) passed from the cranial cavity through this opening into the cavum epiptericum (e.g., Tra 248). There it ballooned into the Gasserian (trigeminal) ganglion and divided into the ophthalmic (V_1), maxillary (V_2), and mandibular (V_3) branches of the trigeminal nerve (Oelrich, 1956).

The otic capsule is an expansive, voluminous spherical chamber that dominates the back of the skull. A large jugular recess is excavated into the capsule beneath the horizontal (lateral) semicircular canal (Fig. 18A). It opens anterolaterally, but the opening was probably covered in life by a cluster of temporal scales as in *Rhineura floridana* (Eigenmann, 1902). The dorsal edge of the jugular recess is bounded by the paroccipital process, which encloses the horizontal semicircular canal. The fenestra ovale opens into the roof of the jugular recess just below the paroccipital process (Fig. 3I). The footplate of the stapes sits within the fenestra ovale, but whether it completely filled or overlapped the rim of the foramen is unclear due to postmortem displacement of both stapes. The facial foramen pierces the prootic (Figs. 3H, 18A) where the trunk of cranial nerve VII exited the cranial wall into the jugular recess.

The occipital recess is an excavation between the posterior part of the otic capsule and the occipital condyle (Fig. 18B). Within the occipital recess lies the vagus foramen (Tra 379) that transmitted the glossopharyngeal (IX) and vagus (X) nerve trunks and the internal jugular vein. Also opening into the occipital recess is the smaller hypoglossal foramen (Tra 384) that transmitted branches of the hypoglossal nerve (XII). Both the vagus and hypoglossal foramina follow direct routes laterally from the cranial cavity as they pierce the cranial wall, opening into the same large hole in the occipital recess.

Occipital complex. Ontogenetic series of *Amphisbaena* (Montero et al., 1999) indicate that the supraoccipital, paired exoccipital, and basioccipital arise separately but fuse together early in osteogenesis to form the occipital complex. As in other squamate reptiles, the basioccipital contributes to the floor of the braincase, the exoccipitals to its walls, and the supraoccipital to its roof.

The basioccipital portion of the occipital complex forms the most posterior portion of the braincase floor between the otic capsules as well as the median portion of the occipital condyle. The dorsal surface of the basioccipital is smooth and forms a slightly arched floor beneath the hindbrain (Figs. 3J, 4B,C). The occipital condyle (Fig. 18C) is very broad and presents a heterocoelous or dumbbell-shaped articular surface. The basioccipital and exoccipitals con-

tribute to the occipital condyle (Montero et al., 1999), as in squamates generally, although no sutures remain evident in this specimen. The supraoccipital portion of the occipital complex forms the roof of the foramen magnum, the posterior part of the braincase, and the dorsal portion of the otic complex. The foramen magnum opens posteriorly and is not elevated. Looking into the foramen magnum (Fig. 6E), the dorsal portion of the cranial cavity is largely filled by the projecting dorsomedial walls of the otic capsules.

Internal anatomy of otic–occipital complex (Fig. 3). The internal morphology of the endocranium and otic capsule can be best appreciated by describing its geometry from anterior to posterior with reference to representative transverse CT sections. Anteriorly (Tra 136) (Fig. 3C) the cranial cavity is roughly heart-shaped and completely enclosed by the descending processes of the frontals. More posteriorly (Tra 185) (Fig. 4B) the cranial cavity is roofed by the ventral surface of the parietal and floored by the orbitosphenoids. About midway back through the skull (Tra 194) the temporal laminae of the parietal meet the orbitosphenoids to exclude the descending processes of the frontals from the endocranial wall. Further posteriorly (Tra 203) the anterior superior processes of the alar processes of the prototics separate the temporal laminae of the parietal from the orbitosphenoids. The alar processes gradually (by Tra 244) (Fig. 5A) form most of the lateral wall of what is now a dorsoventrally elongated cranial cavity. The alar processes then divide (Tra 246) to form the dorsal and anteroventral margins of the Gasserian foramina. Shortly after this (Tra 276) the anterior Vidian foramina pierce the parabasisphenoid at the proximal corners of the basipterygoid processes. Just before the closure of the Gasserian foramina (Tra 294) (Fig. 3G) the internal carotid canals open into the floor of the cranial cavity.

Further posteriorly (Tra 308) (Figs. 3H, 5A) the cranial cavity becomes constricted dorsally by the expansion of the otic capsules. Just posterior to the basipterygoid processes of the parabasisphenoid, the Vidian canals perforate the parabasisphenoid via the posterior Vidian foramina (Tra 299), the facial foramina pierce the cranial cavity from the jugular recesses (Tra 308), and the anterior auditory foramina pierce the cranial cavity from the vestibules of the otic capsules (Tra 309) (Fig. 5C). Further posteriorly (Tra 316) the cranial cavity becomes even more constricted dorsally with the medial walls of the otic capsules forming almost right angles. This constriction is most pronounced at the widest point of the otic–occipital complex (Tra 327) (Fig. 3I). Here, two laterally paired foramina pierce the cranial cavity from the vestibules: the posterior auditory foramina from their ventromedial corners and the endolymphatic canals (Fig. 5A) from their dorsomedial walls.

Just posterior to the fenestrae ovali, at the point where the foramen magnum begins to open dorsally (Tra 366) (Fig. 3J), the recessus scalae tympani mark the entrance of the perilymphatic ducts into the ventrolateral corners of the cranial cavity. Further posteriorly (Tra 378) the vagal foramina pierce the cranial cavity, opening into the occipital recesses; slightly posterior to this (Tra 384) the hypoglossal foramina do the same.

Moving back to the anterior end of the otic complex, the anterior vertical semicircular canal opens just posterior to the midpoint of the Gasserian foramen (Tra 279) (Figs. 3G, 5A). It emerges from the anterior end of the anterior ampullary recess and abruptly turns posterodorsally (Fig. 4A), eventually meeting the recessus crus communis (Tra 322) (Figs. 3I, 4B). Just ventral to the anterior ampullary recess opens the anterior elbow of the perilymphatic duct (Tra 286) (Figs. 3G, 4A). This duct takes a somewhat tortuous route ventromedially for almost the entire length of the otic capsule (to Tra 378) (Fig. 5B,C), eventually looping back anteriorly to open into the cranial cavity via the recessus scalae tympani (Tra 359) (Fig. 3J).

Further posteriorly, at the level of the posterior opening of the Vidian canal (Tra 302) (Fig. 3H), the external semicircular canal emerges laterally from the anterior ampullary recess and curves posteriorly (Fig. 5A), where it eventually enters the posterior ampullary recess (Tra 381). Just behind the posterior Vidian foramen the anterior auditory foramen passes from the vestibule to the cranial cavity (Tra 309) (Fig. 3H). At about the same place lies the anterior edge of the statolith mass, an ovoid calcified body that expands posteriorly to fill roughly half of the vestibule (Figs. 3I, 5A).

Just anterior to the widest point of the otic–occipital complex, the perilymphatic duct opens into the jugular recess (Tra 316). Slightly posterior to this (Fig. 3I) the anterior vertical semicircular canal opens dorsally into the recessus crus communis (Tra 321) (Fig. 4B), the fenestra ovale opens into the jugular recess (Tra 324), and the posterior auditory foramen (Tra 322) and endolymphatic canal (Tra 328) exit the vestibule medially to enter the cranial cavity. At the level of flattening of the occipital crest of the supraoccipital the fenestra ovale closes (Tra 353). Further posteriorly (Fig. 3J) the perilymphatic duct opens briefly into the vestibule (Tra 359) (Fig. 5B) and the posterior vertical semicircular canal emerges dorsally from the recessus crus communis (Tra 362) (Fig. 5B) and ventrally from the vestibule (Tra 374). This point of entry of the perilymphatic duct lies dorsal to the recessus scala tympani through which the perilymphatic duct eventually empties into the cranial cavity after looping further posteriorly. At the posterior end of the otic capsule, at a level between the passages of the vagus (Tra 378) and hypoglossal (Tra 384) canals, the horizon-

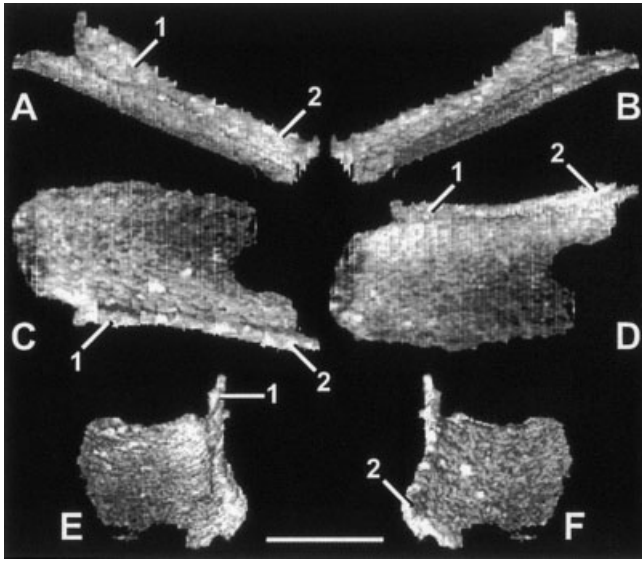


Fig. 19. Left orbitosphenoid in (A) lateral, (B) medial, (C) dorsal, (D) ventral, (E) anterior, and (F) posterior views. Scale bar = 1 mm. 1, ridge clasped by orbitosphenoid process of medial lamina of descending process of frontal; 2, ridge clasped by temporal lamina of parietal.

tal semicircular canal enters the posterior ampullary recess (Tra 380).

Orbitosphenoid (Fig. 19; Tra 176–243). In most squamates the orbitosphenoid is a small, paired, arched element that curves around the posterior margin of the optic foramen. In contrast, in many amphisbaenians the orbitosphenoids are fused, greatly enlarged, and possibly augmented by a membranous component (Zangerl, 1944; Bellairs and Gans, 1983; Montero et al., 1999). In these species the azygous, platelike orbitosphenoid is exposed in lateral view and pierced by greatly reduced optic foramina. The unique condition of this element in *Amphisbaena alba* led Montero and Gans (1999) to suggest that it is not homologous to the orbitosphenoid in other squamates and to propose the term “tabulosphenoid.” However, small paired orbitosphenoids were described in the “shovel-headed” amphisbaenian *Monopeltis* (see Kritzing, 1946). In *Rhineura hatcherii* no tabulosphenoid-like element exists. Instead, the parabasisphenoid is greatly expanded laterally and paired elements like those in *Monopeltis* lie above the medial laminae of the descending processes of the frontal (Fig. 3E,F). We follow Kritzing (1946) in referring to these elements as orbitosphenoids.

In this specimen of *Rhineura hatcherii*, the left orbitosphenoid is much better preserved than is the right. The orbitosphenoid lines the dorsal surface of the medial lamina of the descending process of the frontal (Figs. 3E, 4B). It is dorsally inclined (Fig. 19A), paralleling the angle of the parabasisphenoid. It is almost rectangular (Fig. 19C), slightly concave dorsally, thicker laterally than medially, and lies in

close medial apposition with its opposite throughout its length.

The orbitosphenoid is clasped anteriorly by the orbitosphenoid process of the medial lamina of the descending process of the frontal (Figs. 4B, 19C). More posteriorly (Tra 193) the lateral edge of the orbitosphenoid is held by the ventral edge of the temporal lamina of the parietal; a slight longitudinal ridge marks this contact (Fig. 19C). Further posteriorly (Tra 204) it is separated from the temporal lamina of the parietal by the anterior superior process of the alar process of the prootic. The orbitosphenoid terminates posteriorly just before the opening of the Gasserian foramen. There are no optic foramina.

Quadrate (Fig. 20; Tra 264–316). The quadrate in squamate reptiles is a paired element that links the mandible to the braincase, with a synovial articulation at either end providing for a streptostylic articulation. In *Rhineura hatcherii* the quadrate is short, stout, and complexly shaped. The shaft is narrower than either the distal mandibular condyle or the proximal cephalic condyle. The quadrate is inclined anteriorly at an angle of almost 45° relative to the long axis of the skull (Fig. 6A).

The cephalic condyle of the quadrate articulates posterodorsally with the squamosal/paroccipital

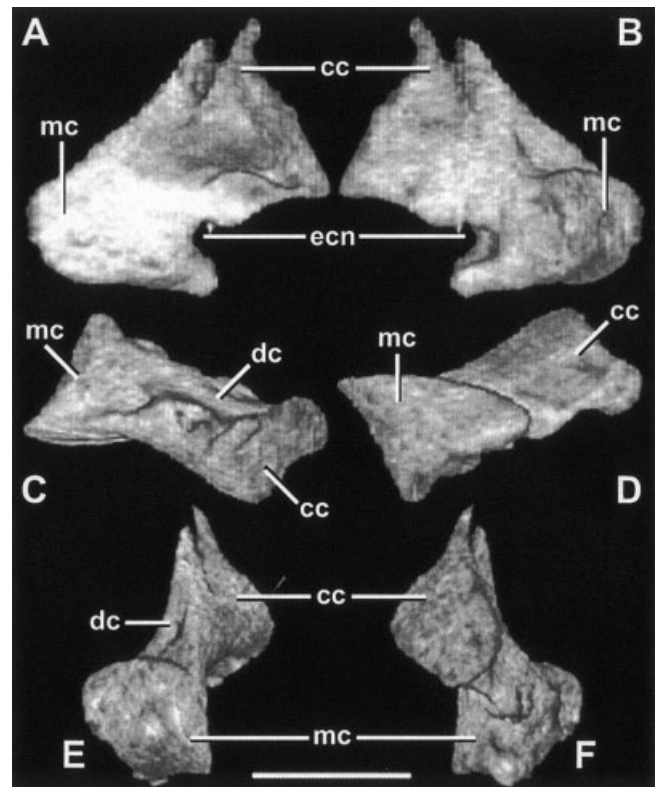


Fig. 20. Right quadrate (inverted) in (A) lateral, (B) medial, (C) dorsal, (D) ventral, (E) anterior, and (F) posterior views. Scale bar = 1 mm. cc, cephalic condyle; dc, dorsal crest; ecn, extracolumellar notch; mc, mandibular condyle.

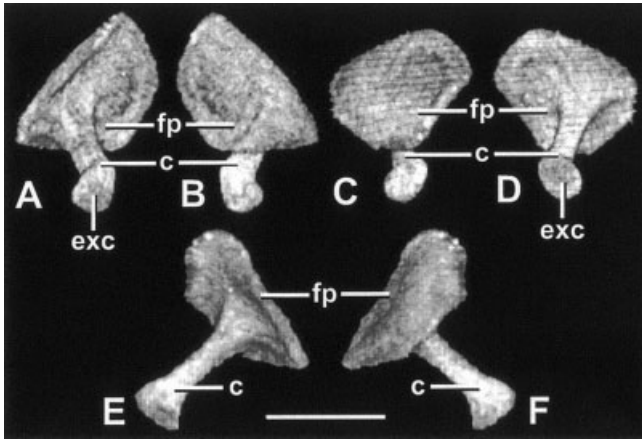


Fig. 21. Right stapes (inverted) in (A) lateral, (B) medial, (C) dorsal, (D) ventral, (E) anterior, and (F) posterior views. Scale bar = 1 mm. c, columella; fp, footplate; exc, possible extracolumellar attachment surface.

process and the mandibular condyle forms a saddle-shaped articulation anteroventrally with the glenoid fossa of the mandible (Fig. 6A). A vertical ridge, the dorsal crest, runs dorsoventrally along the quadrate (Fig. 20C) beginning at the cephalic condyle, gradually flattening out, and disappearing before reaching the mandibular condyle. This crest divides the quadrate into halves. The quadrate process of the pterygoid extends posterodorsally to tightly wrap around the ventromedial surface of the quadrate (e.g., Tra 294) (Fig. 5C). The posteroventral margin of the quadrate is notched where it receives the extracolumella (Fig. 20A,B). In most extant amphisbaenians an extracolumella extends anteriorly across the lateral aspect of the quadrate, attaching to soft tissue along the mandible (Gans and Wever, 1972, 1975; Gans, 1978). Each quadrate exhibits one or more irregularly placed nutritive foramina (Figs. 3H, 5C).

Stapes (Fig. 21; Tra 300–349). The columellar auris in squamates includes the bony stapes and cartilaginous extracolumella (Romer, 1956). In this specimen the left stapes was displaced postmortem entirely into the vestibule (Fig. 3I). The right stapes, which is only slightly displaced, serves as the basis for this description. The basal footplate is large and subcircular (Fig. 21C) and fits into the deeply recessed fenestra ovale in life. Its anterodorsal rim is rolled laterally, a feature previously unreported in amphisbaenians. A long, hollow, rodlike columella arises from the lateral face of the footplate slightly anteroventral to its center (Fig. 21A). The columella extends ventrolaterally almost to the quadrate (Fig. 5C), terminating distally in a flattened oval disk with a dimpled surface (Fig. 21A) that probably attached to a cartilaginous or partially ossified extracolumella, as in most extant amphisbaenians.

Overview of Mandible (Fig. 22)

The lower jaw in *Rhineura hatcherii* consists of two rami that were likely loosely joined anteriorly in a fibrous symphyseal articulation and that articulate posteriorly with the quadrates. Each ramus curves anteromedially to meet its opposite in a deep, flat articular surface. The mandible exhibits an angulation that parallels the craniofacial angulation of the skull (Fig. 6A). A deep, posterodorsally facing U-shaped glenoid fossa receives the mandibular condyle of the quadrate, which has an anterolateral orientation. A posteroventrally projecting, well-developed retroarticular process lies posterior to this articulation. The mandible exhibits several mental foramina running along the anterior half of

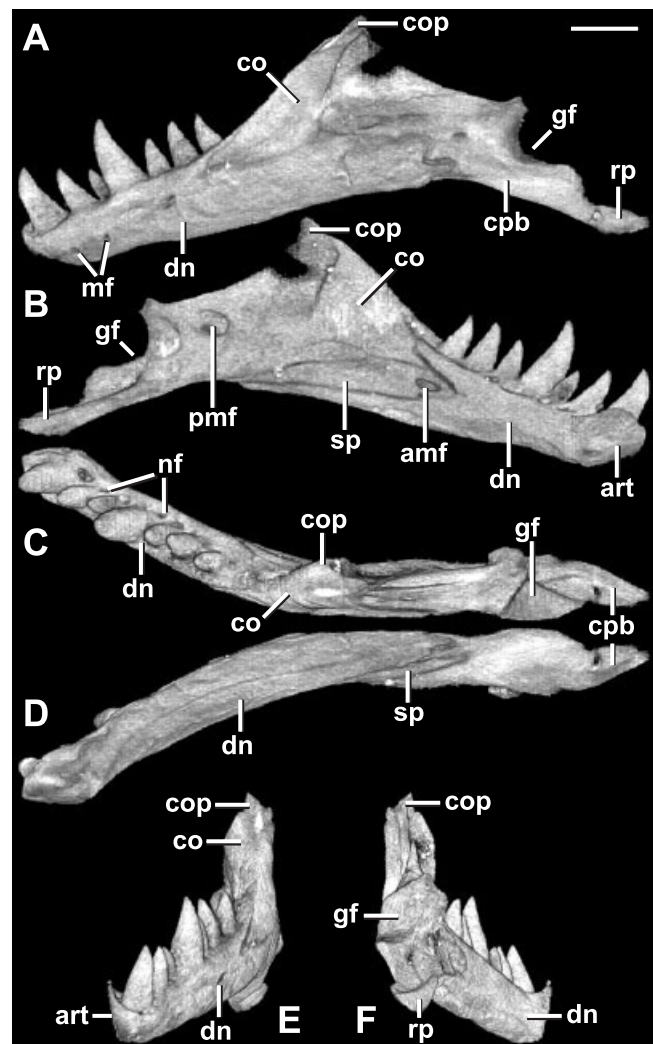


Fig. 22. Right mandible (inverted) in (A) labial, (B) lingual, (C) dorsal, (D) ventral, (E) anterior, and (F) posterior views. Scale bar = 1 mm. amf, anterior mylohyoid foramen; art, articular surface; co, coronoid; cop, coronoid process; cpb, compound bone; dn, dentary; gf, glenoid fossa; mf, mental foramen; nf, nutritive foramen; pmf, posterior mandibular foramen; rp, retroarticular process; sp, splenial.

the dentary, indicating cutaneous vascularization and innervation. The Meckelian canal is a closed tube, its walls formed mainly by the dentary laterally and the splenial medially.

In squamates, the mandible typically comprises six elements that form a tubular canal: dentary, coronoid, surangular, angular, splenial, and articular. In most amphisbaenians the postdentary elements exhibit significant fusion, resulting in a compound postdentary bone (Fig. 22A). In most rhineurids there are five distinct elements: dentary, coronoid, compound bone, and two additional postdentary elements (Berman, 1973). In this specimen of *Rhineura hatcherii* there are four distinct elements: dentary, coronoid, compound bone, and one additional postdentary bone. Montero and Gans (1999) interpreted an isolated postdentary element in *Amphisbaena alba* as the angular, whereas Berman (1973, 1976) interpreted one in several rhineurids as the splenial. In squamates the splenial typically lies entirely on the lingual surface of the mandible, its anterior end lining the Meckelian canal. The angular typically is a ventral element, with its posterior end exposed on the labial surface of the mandible and its anterior end exposed on the lingual surface. It is difficult to interpret the single postdentary element in *R. hatcherii* as it exhibits characteristics of both the splenial and angular. With this caveat, we refer to this element as the splenial based on its predominantly lingual exposure and deep penetration of the dentary.

The coronoid process is the tallest element in the mandible of *Rhineura hatcherii*. It is formed mainly by the coronoid, with minor contributions from the coronoid process of the dentary and the dorsal edge of the compound bone. The coronoid caps these dorsally and also extends ventrally.

Individual Elements of Mandible

Dentary (Fig. 23; Tra 067–248). In lizards the dentary is the only tooth-bearing bone of the lower jaw and typically constitutes more than half the length of the mandibular ramus (Romer, 1956). The dentary in *Rhineura hatcherii* bears seven subpleurodont teeth along its dorsal margin, the first and fourth being the largest and about equal in size. The teeth have bulbous, hollow bases and their crowns are conical in shape, with the largest teeth slightly recurved and the smaller ones straighter. Just posterior to the first tooth a small subdental shelf extends medial to the tooth row. Nutritive foramina are present along the subdental shelf at the base of each tooth (Figs. 3C, 23C).

The dentary conveys along its length a wide Meckelian canal (Figs. 3C, 4A) that transmitted the inferior alveolar nerve and artery. Multiple mental foramina penetrate the labial surface of the dentary (Fig. 23A), where they transmitted cutaneous branches of the inferior alveolar nerve to the skin.

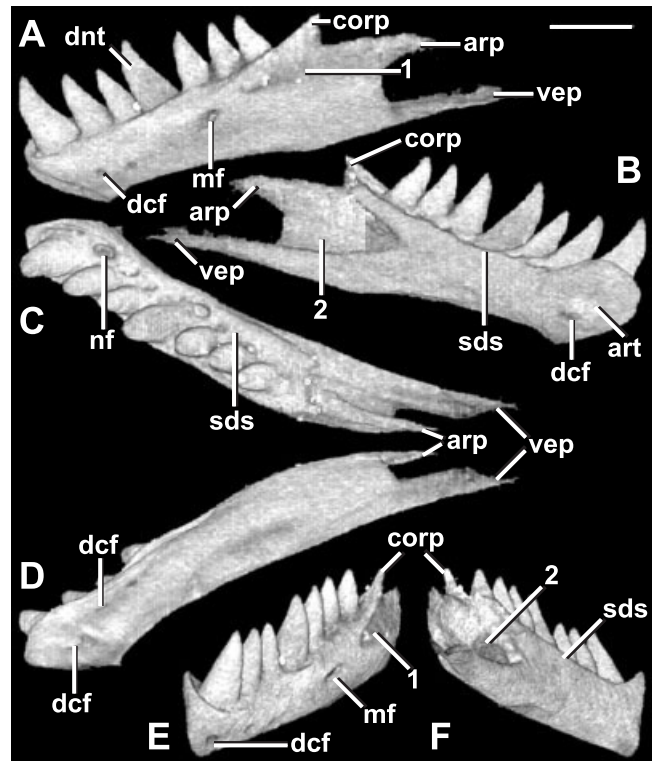


Fig. 23. Left dentary in (A) labial, (B) lingual, (C) dorsal, (D) ventral, (E) anterior, and (F) posterior views. Scale bar = 1 mm. arp, articular process; art, articular surface; corp, coronoid process; dcf, dentary communicating foramen; dnt, dentary tooth; mf, mental foramen; nf, nutritive foramen; sds, subdental shelf; vep, ventral process; 1, area of overlap by anterolateral process of coronoid; 2, area of overlap by coronoid, splenial, and compound bone.

The Meckelian canal terminates anteriorly in front of the first tooth (Tra 098) where it splits into three communicating foramina: one branches laterally to the labial surface of the dentary (Tra 095) (Fig. 23A); one branches medially to the articular face (Tra 091) (Fig. 23B); and one branches ventrally to its inferior edge (Tra 086) (Fig. 23E).

At the anterior end of the dentary (Fig. 23B) the articular surface is vertically oriented, broader dorsally than ventrally, and slightly pointed at its posteroventral margin. Three processes project from the rear part of the dentary (Fig. 23A). The dorsalmost is the coronoid process, which projects posterodorsally from just behind the last dentary tooth. It is mediolaterally compressed and sandwiched between the anterolateral and anteromedial processes of the coronoid bone (e.g., Tra 164) (Fig. 5C); overlap by the anterolateral process of the coronoid is delimited by a V-shaped depression (Fig. 23A). Below the coronoid process of the dentary is the articular process, which projects posteriorly in the direction of the craniomandibular articulation almost to the level of the coronoid process of the mandible. It is also mediolaterally compressed and lies along the labial surface of the compound bone (Fig. 3E). The

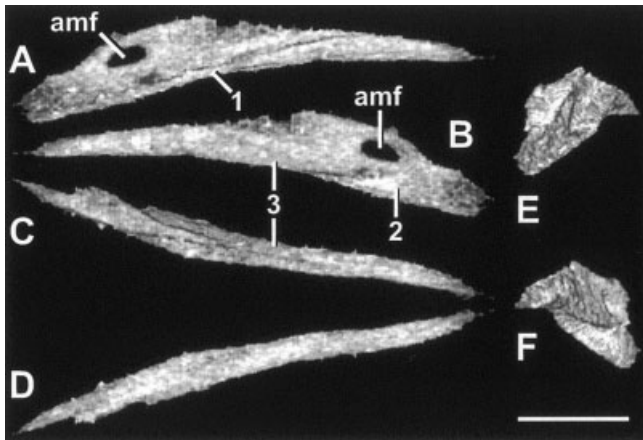


Fig. 24. Left splenial in (A) labial, (B) lingual, (C) dorsal, (D) ventral, (E) anterior, and (F) posterior views. Scale bar = 1 mm. amf, anterior mylohyoid foramen; 1, ridge clasped by compound bone; 2, area of overlap by dentary; 3, exposed surface.

third process of the dentary, the ventral process, projects posteriorly along the inferior edge of the mandible (Fig. 22D) to the level of the Gasserian foramen. It is dorsoventrally compressed and clasps the ventral margin of the splenial and the compound bone (Fig. 3F).

The dentary articulates posteriorly with the splenial, coronoid, and compound bone via a large V-shaped excavation (Figs. 3D, 23B). A gracile process of the splenial inserts deeply into the Meckelian canal (Fig. 4A), lining its medial surface (Fig. 3C) and terminating at the level of the sixth tooth (Tra 134). At the level of the seventh tooth, the anteromedial process of the coronoid (Tra 143) and the dentary process of the compound bone (Tra 144) also insert into the Meckelian canal (Fig. 5C), lining its dorsal and lateral surfaces, respectively. As a result, the dentary is completely excluded from the walls of the Meckelian canal from approximately transverse slice 151 posteriorly.

Splenial (Fig. 24; Tra 132–249). The splenial is a thin, flattened bony plate lying within a recess of the dentary and located entirely on the medial and ventral surfaces of the mandible (Fig. 22B). A distinct splenial is absent in many amphisbaenians but often is present in rhineurids (Berman, 1973, 1976). The splenial is obscured from view anteriorly by the dentary, lining the medial wall of the Meckelian canal (Figs. 3C, 4A) to the level of the sixth dentary tooth; this area of overlap is delimited by a depression on the anteromedial surface of the splenial (Fig. 24B). At the posterior edge of the seventh dentary tooth (Tra 148) the splenial becomes exposed on the medial surface of the mandible (Figs. 3D, 22B). At this point the splenial articulates with the anteromedial process of the coronoid dorsally and the dentary process of the compound bone ventrally, and together these three elements line the walls of the Meckelian canal. Just posterior to the seventh den-

tary tooth (Tra 156) the splenial is pierced by the anterior mylohyoid foramen (Fig. 24A), which transmitted the anterior mylohyoid nerve (Oelrich, 1956). Behind this foramen the contact of the splenial and anteromedial process of the coronoid is exposed on the medial surface of the mandible. The splenial tapers dorsoventrally and becomes excluded from the wall of the Meckelian canal by the compound bone just anterior to the apex of the coronoid process (Tra 172) (Fig. 3E). As the splenial tapers posteriorly to a point it gradually migrates ventrally to lie within a groove on the compound bone (e.g., Tra 229) (Fig. 22D).

Coronoid (Fig. 25; Tra 143–254). The coronoid is a robust triradiate element in *Rhineura hatcherii*. It projects dorsally into a tall, posteriorly inclined coronoid process that reaches the midpoint of the orbit when the jaw is closed (Figs. 5A, 6A). In most extant amphisbaenians the dentary overlaps the coronoid, but in rhineurids the reverse is true (Kearney, 2003). In *R. hatcherii* the coronoid straddles the dorsal surface of the mandible via two anterior processes that extend roughly to the level of the posteriormost dentary tooth. A posterior process extends predominantly on the medial surface of the mandible to a point two-thirds of the distance between the

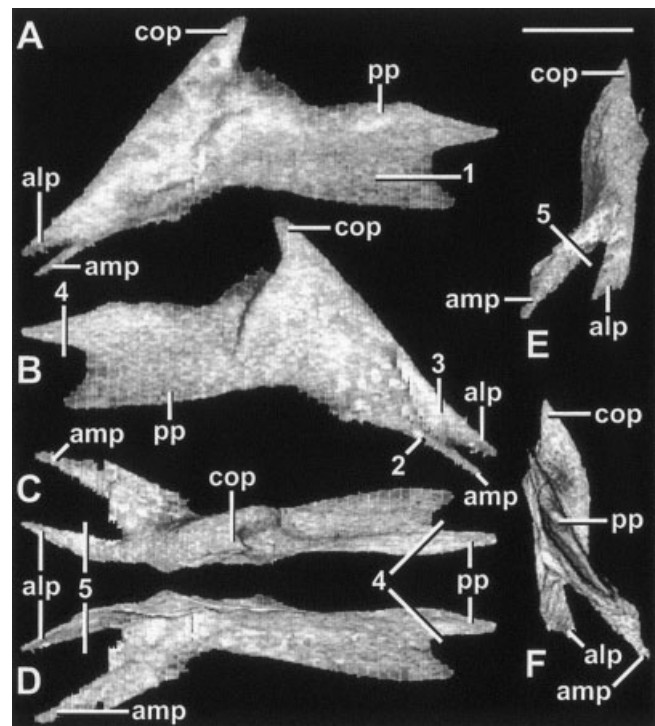


Fig. 25. Left coronoid bone in (A) labial, (B) lingual, (C) dorsal, (D) ventral, (E) anterior, and (F) posterior views. Scale bar = 1 mm. alp, anterolateral process; amp, anteromedial process; cop, coronoid process; pp, posterior process; 1, area of overlap by compound bone; 2, area of overlap by dentary; 3, area overlapping dentary; 4, anterior margin of posterior mandibular foramen (in compound bone); 5, groove that receives coronoid process of dentary.

apex of the coronoid process and the glenoid fossa (Fig. 22B).

The anterolateral and anteromedial processes of the coronoid (Fig. 25A) together clasp the coronoid process of the dentary anteriorly (e.g., Tra 162) (Fig. 5C) and terminate in pointed tips. The anteromedial process initially penetrates the dentary (Tra 143) to briefly contribute to the dorsomedial margin of the Meckelian canal, but posteriorly (Tra 148) it is excluded from the wall of the Meckelian canal by the splenial and compound bone (Fig. 3D). The anterolateral process lies within a shallow depression on the dorsolateral surface of the dentary (Figs. 3C, 22A). The posterior process of the coronoid is a mediolaterally flattened, bladelike process that lines the medial surface of the compound bone (Fig. 3F). This process terminates in a U-shaped prong (Fig. 25B) that parallels the anterior margin of the posterior mandibular foramen in the compound bone (Fig. 22B).

Compound bone (Fig. 26; Tra 144–324). The compound postdentary bone presumably incorporates the fused supraangular, articular, prearticular, and splenial in most amphisbaenians (Montero and Gans, 1999; Montero et al., 1999). However, in *Rhineura hatcherii* a discrete splenial is present as interpreted here. The compound bone is the most posterior element of the mandible. It exhibits an anterior dentary process and a posterior articular process that terminates in a small posteromedially directed retroarticular process. The compound bone contacts the dentary, coronoid, splenial, quadrate, and pterygoid.

The dentary process of the compound bone is deeply incised anteriorly to form lingual and labial blades (Fig. 26C) that insert deeply into the posterior opening of the Meckelian canal in the dentary (Fig. 5C). The lingual blade of the dentary process extends anteriorly almost to the anterior mylohyoid foramen (Tra 167), and posteriorly it gradually excludes the splenial from the medial wall of the Meckelian canal (Tra 173). The labial blade of the dentary process extends even further anteriorly, just past the initial exposure of the splenial on the medial surface of the mandible (Tra 144), to form the labial wall of the Meckelian canal. The blades meet and form a thin tubular sheath that lines the Meckelian canal (Figs. 3E, 5C). The articular process of the compound bone gives rise to a deep U-shaped glenoid fossa posteriorly (Fig. 26C), which is oriented posterolaterally to receive the anteromedially oriented mandibular condyle of the quadrate. Ventromedial to the glenoid fossa the articular process contacts the quadrate process of the pterygoid (Tra 272) (Fig. 5C), then extends posteriorly to form a ventrally deflected retroarticular process that terminates in a blunt tip. This process approaches “Element X” of the otic–occipital complex (Fig. 3H).

The dorsomedial surface of the compound bone is pierced by the posterior mandibular foramen (Tra

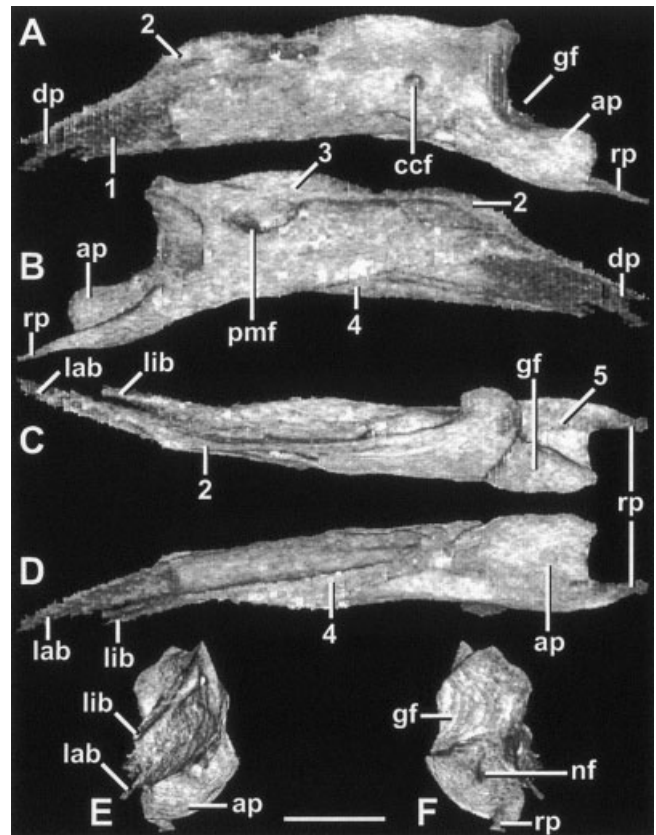


Fig. 26. Left compound bone in (A) labial, (B) lingual, (C) dorsal, (D) ventral, (E) anterior, and (F) posterior views. Scale bar = 1 mm. ap, articular process; ccf, compound bone communicating foramen; dp, dentary process; gf, glenoid fossa; lab, labial blade of dentary process; lib, lingual blade of dentary process; nf, nutritive foramen; pmf, posterior mandibular foramen; rp, retroarticular process; 1, area of overlap by dentary; 2, ridge clasped between coronoid bone and articular process of dentary; 3, area of overlap by posterior process of coronoid; 4, groove for splenial; 5, surface of pterygoid articulation.

247) just anterior to the glenoid fossa (Fig. 26B). This passageway has a small opening directly opposite on the labial surface (Fig. 26A) before continuing anteriorly to open into the Meckelian canal. Numerous canals can be discerned within the articular process (e.g., Tra 264) and its posteroventral surface is pierced by a nutritive foramen (Fig. 26F).

DISCUSSION

Gans and co-workers (Gans, 1960, 1974, 1978; Montero and Gans, 1999; Montero et al., 1999) have commented extensively on the many anatomical peculiarities that presumably are related to the fossorial habits of *Rhineura* and other amphisbaenians. Because amphisbaenians use their heads as digging tools, their skulls are highly modified. Gans discussed how contacts between cranial elements are often extremely complex, with interlocking and interdigitating sutures and significant overlap of

bones. This is in contrast to most squamates, in which the majority of cranial elements articulate in simple abutting contacts. The present study of *R. hatcherii* offers an even more thorough examination of a single specimen via the power of HRXCT, and our new observations largely corroborate and extend many of Gans' earlier interpretations, at least so far as *Rhineura* is concerned.

The skull is divisible into fundamentally distinct facial and cranial segments, and their individuality is revealed by the different ways in which their parts comprise wholes. In the otic–occipital complex, the individual elements are fused to a degree exceeding any other amphisbaenian yet described. In contrast, in the facial region of the skull there is little in the way of secondary fusion between elements. The facial elements remain discrete throughout life, but are connected via elaborate, fibrous diarthroses that may leave the elements slightly flexible with respect to one another and to the otic–occipital region.

It is helpful in understanding the two skull regions to compare and contrast them with respect to their mechanical organization. The rigid cranial segment contributes to the protection, stability, and acuity of all neurosensory systems of the head and the feeding apparatus, while transmitting forces between the face and body. One set of forces is that generated by the mandibular adductor musculature. The large sagittal crest of the supraoccipital and parietal and the robust architecture of the mandible suggest that relatively strong bite forces could be generated. Serial sections of living species (e.g., Eigenmann, 1902; Montero and Gans, 1999) indicate extensive development of jaw adductor musculature. Moreover, the mandible and quadrate are organized in a mechanical configuration that would maximize bite force (Gans, 1960).

The facial segment is subjected to both high complex loads and complex torques and, in response, is organized as a series of imbricating processes and laminae of bone that are held together by an exceptionally elaborate system of interosseous ligaments and synovial joints. The fact that the boundaries between each facial bone are so distinctive in this fossilized specimen suggests the presence in life of the thick, ligamentous, interosseous bands that can be observed in serial sections of extant specimens (Gans, 1960).

The facial segment as a whole is suspended from the otic–occipital complex dorsally by the tortuous frontoparietal suture. The facial segment might accommodate a slight degree of anteroposterior compression via dorsoventral flexion at the frontoparietal suture and potential ventral movement at the synovial basipterygoid articulation. The organization of the complex cranio-quadrate and quadrate-mandibular joints may also reflect burrowing forces to some degree.

A second striking observation that *Rhineura hatcherii* presents is the extreme elaboration of its

cranial sensory organs. The effects of scaling have yet to be fully measured, but the brain would appear to have filled the cranial cavity. Although eyes were absent, the cranial cavity suggests large olfactory bulbs were present and supplied extensive olfactory epithelium that ran across the relatively voluminous nasal cavity. This interpretation is supported by studies of living species (Gabe and Saint Girons, 1976; Schwenk, 1993). The large cavum epiptericum and extensive system of trigeminal communicating foramina over the face suggest that the face served as a tactile organ of exceptional acuity compared to that of most squamates. The otic region is quite large and both hearing and vestibular reception were highly derived. The cerebellar region of the cranial cavity appears relatively poorly developed.

Four basic cranial shapes are exhibited by amphisbaenians—"round-headed," "shovel-headed," "keel-headed," and "spade-headed" (Gans, 1974)—each purportedly correlated with a stereotyped digging behavior. How the elements of the skull are modified with respect to these four basic morphotypes is of interest, both functionally and phylogenetically. The only other amphisbaenian whose cranial anatomy has been described in comparable detail is *Amphisbaena alba* (see Montero and Gans, 1999). Here we briefly compare and contrast the skull of the shovel-headed *Rhineura hatcherii* with that of the round-headed *A. alba*. Ultimately, our goal is to compare and contrast all four morphotypes based on HRXCT data to assess the three-dimensional modifications accompanying the evolution of each cranial shape/digging mode.

The most striking difference between the skulls of *Amphisbaena alba* and *Rhineura hatcherii* is the strong craniofacial angulation and depressed snout of the latter versus the small degree of angulation and the rounded snout of the former. In *A. alba* the front of the snout forms a blunt, smoothly convex surface. The nasal process of the premaxilla is long and narrow at the rounded anterior edge of the snout. In *R. hatcherii* the premaxilla is dorsoventrally flattened, forming a spatulate digging wedge at the front of the snout. The premaxilla also exhibits two robust palatal processes in *R. hatcherii* that are absent in *A. alba*. The premaxilla is, in general, a much stouter element in *R. hatcherii*. In *A. alba* the superficial sutures between the elements of the snout are deeply lobate and intricate, whereas in *R. hatcherii* they only weakly interdigitate by comparison. This difference presumably reflects the different types of mechanical forces imparted by different digging modes. The position of the external nares differs dramatically in the two species as well, opening ventrally in *R. hatcherii* but anterolaterally in *A. alba*. This difference most likely is due to the use of the spatulate snout as a shovel in *R. hatcherii*.

The facial region of the skull in *Amphisbaena alba* is much shorter than that in *Rhineura hatcherii*, and the skull is narrower overall. Reflecting this

difference, the maxilla of *A. alba* is much shorter and lacks the extensive orbital process present in *R. hatcherii*.

Ventrally, the premaxillary teeth are located just at the anterior rim of the snout in *Amphisbaena alba*, whereas in *Rhineura hatcherii* the premaxillary dentition is displaced posteriorly from the edge of the snout by the rostral process and the ventral location of the nares. Also, the snout is prognathous in *R. hatcherii*, with the premaxilla significantly overhanging the lower jaw and forming a large horizontal rostral blade anterior to the premaxillary dentition. It is questionable whether the premaxillary dentition is functional in *R. hatcherii* due to this condition, which may also explain the small number of premaxillary teeth in “shovel-headed” forms generally (Kearney, 2003). The number of premaxillary teeth in *A. alba* (seven) contrasts with the three found in *R. hatcherii*, most rhineurids, and many extant “shovel-headed” forms (Zangerl, 1944; Estes, 1983; Kearney, 2003). Thus, remodeling of the anterior portion of the skull into a digging edge may have rendered the premaxillary dentition vestigial in these species.

Unique modifications of the mandible and dentition are also present in “shovel-headed” forms. Following the steep angulation of the facial segment of the skull, the mandible also exhibits an angulation, with a ventrally deflected retroarticular process following the angle of the cranial segment. The mandible is much shorter overall in *Amphisbaena alba* than in *Rhineura hatcherii*, especially the postcoronoid region. Both the coronoid and compound bones are larger, more substantial elements in *R. hatcherii*. The dentition pattern in *A. alba* consists of a high number of premaxillary teeth and a low number of maxillary teeth—the opposite of the pattern in *R. hatcherii*. The number of mandibular teeth in the two species is comparable.

The ventrolateral and paroccipital processes of the otic-occipital complex in *Amphisbaena alba* are greatly reduced as compared to *Rhineura hatcherii*. The back of the skull is also constructed very differently in the two forms. The occipital condyle is much larger and wider in *R. hatcherii* than in *A. alba*. In *R. hatcherii* the occipital condyle is saddle-shaped, whereas it is composed of two small rounded knobs in *A. alba*. The foramen magnum is also relatively larger in *R. hatcherii*. In *A. alba* the foramen magnum is roofed over by a well-developed occipital crest that is only weakly developed in *R. hatcherii*. These differences may relate to the posture of the head during digging: in “shovel-headed” forms the muscles that lift the head originate on the neural arches of the vertebrae and insert on the nuchal tendon, which itself inserts on the anteriorly flattened and triangular deflected portion of the parietal (Gans, 1974).

The difference between *Amphisbaena alba* and *Rhineura hatcherii* in the closure of the braincase is

dramatic. In *A. alba* the large, azygous orbitosphenoid contributes significantly to the anterolateral walls of the braincase, whereas in *R. hatcherii* the orbitosphenoids are small, bilaterally paired elements completely enclosed within the braincase. The similarity of the latter condition to that in *Monopeltis* (Kritzing, 1946) is striking, and suggests detailed similarity of braincase construction in biogeographically disparate “shovel-headed” forms. In contrast to Gans’ (1974, 1978) hypothesis that “shovel-headedness” evolved independently in North American, South American, and African amphisbaenians, Kearney (2003) found that “shovel-headed” amphisbaenians formed a monophyletic group. This conclusion was considered tentative given the possibility that supporting characters could be functionally correlated, but the level of detailed similarity in overall braincase construction between *Rhineura* and *Monopeltis* may support a hypothesis of shared ancestry among at least some “shovel-headed” forms.

The amphisbaenian skull is a highly modified, three-dimensionally complex entity. The extensive overlap and interdigitation of the cranial bones is virtually impossible to appreciate or correctly interpret based on articulated specimens. High-resolution X-ray CT provides a nondestructive means of studying the detailed internal anatomy of these problematic taxa. Further progress in understanding amphisbaenian anatomy and evolution will require comparably detailed studies of more species.

ACKNOWLEDGMENTS

We thank Mike Greenwald for making the specimen available for HRXCT scanning. Scanning was performed by Richard Ketcham. John Weinstein photographed the specimen (Fig. 1A,C). Carl Gans provided valuable assistance with comparative specimens, references, and discussion. Chris Bell, Nate Kley, Olivier Rieppel and Kurt Schwenk provided helpful reviews. Kevin de Queiroz provided helpful discussions regarding braincase structure.

LITERATURE CITED

- Baur G. 1893. The discovery of Miocene amphisbaenians. *Am Nat* 27:998–999.
- Bellairs Ad’A, Gans C. 1983. A reinterpretation of the amphisbaenian orbitosphenoid. *Nature (Lond)* 302:243–244.
- Berman DS. 1973. *Spathorhynchus fossorium*, a Middle Eocene amphisbaenian (Reptilia) from Wyoming. *Copeia* 1973:704–721.
- Berman DS. 1976. A new amphisbaenian (Reptilia: Amphisbaenia) from the Oligocene-Miocene John Day Formation, Oregon. *J Paleo* 50:165–174.
- Cope ED. 1900. Crocodylians, lizards and snakes of North America. *Ann Rep US Nat Mus* 1898:153–1270.
- deBeer GR. 1937. The development of the vertebrate skull. Oxford: Oxford University Press.

- Eigenmann CH. 1902. The eyes of *Rhineura floridana*. Wash Acad Sci Proc 4:533–548.
- Estes R. 1983. Sauria terrestria, Amphisbaenia. Handbuch der Paläoherpetologie, Teil 10A. Stuttgart: Gustav Fischer Verlag.
- Estes R, de Queiroz K, Gauthier J. 1988. Phylogenetic relationships within Squamata. In: Estes R, Pregill G, editors. Phylogenetic relationships of the lizard families: essays commemorating Charles L. Camp. Stanford: Stanford University Press. p 119–281.
- Gabe M, Saint Girons H. 1976. Contribution a la morphologie comparée des fosses nasales et de leurs annexes chez les lépiodosauriens. Mém Mus Nat Hist Nat A98:1–87.
- Gans C. 1960. Studies on amphisbaenids (Amphisbaenia, Reptilia). 1. A taxonomic revision of the Trogonophinae and a functional interpretation of the amphisbaenid adaptive pattern. Bull Am Mus Nat Hist 119:129–204.
- Gans C. 1974. Biomechanics. An approach to vertebrate biology. Philadelphia: JP Lippincott.
- Gans C. 1978. The characteristics and affinities of the Amphisbaenia. Trans Zool Soc Lond 34:347–416.
- Gans C, Wever E. 1972. The ear and hearing in Amphisbaenia (Reptilia). J Exp Zool 179:17–34.
- Gans C, Wever E. 1975. The amphisbaenian ear: *Blanus cinereus* and *Diplometopon zarudnyi*. Proc Natl Acad Sci USA 72:1487–1490.
- Gilmore CW. 1928. Descriptions of new and little-known fossil lizards from North America. Proc US Nat Mus 86:11–26.
- Jollie MT. 1960. The head skeleton of the lizard. Acta Zool 41:1–64.
- Kearney M. 2003. Systematics and evolution of the Amphisbaenia (Reptilia: Squamata) based on morphological evidence from fossil and living forms. Herp Monogr 17:1–74.
- Kesteven L. 1957. Notes on the skull and cephalic muscles of the Amphisbaenia. Proc Linn Soc NSW 82:109–116.
- Kritzinger CC. 1946. The cranial anatomy and kinesis of the South African amphisbaenid *Monopeltis capensis* Smith. S Afr J Sci 42:175–204.
- Lakjer T. 1927. Studien über die Gaumenregion bei Sauriern im Vergleich mit Anamniern und primitiven Sauropsiden. Zool Jahrb (Anat) 49:57–356.
- McMahon T, Bonner JT. 1983. On size and life. New York: Scientific American Library.
- Montero R, Gans C. 1999. The head skeleton of *Amphisbaena alba* Linnaeus. Ann Carn Mus 68:15–80.
- Montero R, Gans C, Lions M. 1999. Embryonic development of the skeleton of *Amphisbaena darwini heterozonata* (Squamata: Amphisbaenidae). J Morphol 239:1–25.
- Oelrich TM. 1956. The anatomy of the head of *Ctenosaura pectinata* (Iguanidae). Misc Publ Mus Zool Univ Mich 94:1–122.
- Olson EC. 1995. Introduction to *Thrinaxodon*, digital atlas of the skull. In: Rowe T, Carlson W, Bortorff W, editors. *Thrinaxodon*: digital atlas of the skull. CD-ROM (2nd ed). Austin: University of Texas Press.
- Patterson C. 1977. Cartilage bones, dermal bones and membrane bones, or the exoskeleton versus the endoskeleton. In: Andrews S, Miles M, Walker AD, editors. Problems in vertebrate evolution. London: Academic Press. p 77–121.
- Rieppel O. 1981. The skull and the jaw adductor musculature in some burrowing scincomorph lizards of the genera *Acontias*, *Typhlosaurus* and *Feylinia*. J Zool 195:493–528.
- Romer AS. 1956. Osteology of the reptiles. Chicago: University of Chicago Press.
- Rowe T. 1986. Homology and evolution of the deep dorsal thigh musculature in birds and other Reptilia. J Morphol 198:327–346.
- Rowe T, Kappelman J, Carlson WD, Ketcham RA, Denison C. 1997. High-resolution computed tomography: a breakthrough technology for Earth scientists. Geotimes 42:23–27.
- Schwenk K. 1993. Are geckos olfactory specialists? J Zool Lond 229:289–302.
- Starck D. 1979. Vergleichende Anatomie der Wirbeltiere auf evolutionsbiologischer Grundlage. Volume 2. Das Skeletsystem Allgemeines, Skeletsubstanzen, Skelet der Wirbeltiere einschließlich Lokomotionstypen. Berlin: Springer-Verlag.
- Taylor EH. 1951. Concerning Oligocene amphisbaenid reptiles. Univ Kansas Sci Bull 34:521–579.
- Vanzolini PE. 1951. Evolution, adaptation and distribution of the amphisbaenid lizards (Sauria: Amphisbaenidae). Thesis, Harvard University, Cambridge, MA.
- Zangerl R. 1944. Contributions to the osteology of the skull of the Amphisbaenidae. Am Mid Nat 31:417–454.